THE INTRAMOLECULAR VIBRATIONS OF THE WATER MOLECULE IN THE LIQUID STATE

by 602

JAGDEESHCHANDRA N. BANDEKAR

M.Sc., Karnatak University, Dharwar, India, 1969

A MASTER'S THESIS

submitted in partial fulfillment of the

requirements for the degree

MASTER OF SCIENCE

Department of Physics

KANSAS STATE UNIVERSITY
Manhattan, Kansas

1970

Approved by:

Major Professor

TABLE OF CONTENTS

THIS BOOK CONTAINS NUMEROUS PAGES WITH ILLEGIBLE PAGE NUMBERS THAT ARE CUT OFF OR MISSING.

THIS IS AS RECEIVED FROM THE CUSTOMER.

THIS BOOK CONTAINS NUMEROUS PAGES WITH DIAGRAMS THAT ARE CROOKED COMPARED TO THE REST OF THE INFORMATION ON THE PAGE.

THIS IS AS RECEIVED FROM CUSTOMER.

LIST OF TABLES

LIST OF FIGURES

I. INTRODUCTION

This thesis describes a simple normal coordinate analysis used to study the frequency distribution of the internal vibrational modes of a water molecule. The experimental information about the frequency distribution comes from measurements in the infrared spectral region from about 1000 to 4000 cm^{-1}.

This introductory chapter is intended to give a brief sketch of the history, the importance and the current status of information available on the structure of water. Chapter II gives an overview of some recent experiments on liquid water. Chapter III outlines a few of the theories of water structure pertinent to our discussion.

Thales (ca 624- ca 565 B.C.) thought that the basic constituent of this universe was water. It was one of the four Aristotelian elements. Aristotle (384-322 B.C.), borrowing the view of Empedocles (ca 500- ca 430 B.C.), held that earth, air, fire, and water were the four elements from which all the earthly things were made [67]. However, the ancient Greeks seemed to be using the term water in a broader sense which implied the liquid state and fluidity [68]. This was in vogue until the late eighteenth century. About 1770, Henry Cavendish burned hydrogen and obtained water, which indicated that water was composed of hydrogen and oxygen. Soon after 1800, John Dalton, the father of atomic theory, assigned the composition HO to water. About 1815 Avagadro deduced the composition to be H_2O. However, this was not widely accepted by most chemists until about fifty years later [69]. The composition H_2O was found to be correct after some period of confusion [70].

At the beginning of his book on water King [71] comments, "Of all the substances that are necessary to life as we know it on earth, water is by

far the most important, the most familiar, and the most wonderful; yet most people know very little about it." It appears to be nearly impossible to describe the liquid water system by a calculation from first principles. This is so, because of its wide array of unusual and anomalous properties. However, ab initio calculations have been reported for water monomers [72] and dimers [73]. Recently, Pulay [74, 75] has made ab initio calculations of force constants and equilibrium geometries of polyatomic molecules in general and of water in particular.

According to Eyring and Jhon [21], "Water is the most common liquid on earth and yet its structure is not clearly understood." In the past, a great number of qualitative and quantitative theories have been proposed to account for its anomalous behaviour and explain its structure. Unfortunately, none of them is completely adequate.

Biology is one of the fields needing a better understanding of water structure. Water and life seem to be inseparable. Some organisms can live without air but apparently none can exist without water. Henderson [77] has emphasized the biological significance of water. Says Magat [103], "I would appeal to the theoreticians to recognize that water is of paramount importance--be it only for biology--and attempts should be made to attempt a theoretical treatment of its structure and properties, even using oversimplified models for the charge distribution in the water molecule, as in the old Bernal and Fowler model." Hechter [78] states that the fundamental problem of biology is the elucidation of the state and structure of water in living cells and that this has implications in such diverse fields as biochemistry, genetics and cryobiology. For the understanding of macromolecular hydration and of many biological reactions, an understanding of the structure of water is fundamental.

This thesis includes the results of a theoretical study of the vibrational frequency distribution of water. A simple model [66] is developed for interpreting the observed frequency distribution by assuming that the relative intensity of a Raman or infrared band at each frequency measures the relative number of oscillators having that particular frequency at any instant. Equations for potential and kinetic energies of a bent XYZ molecule are developed. The effect of the nearest oxygen atom of the neighbouring molecule on vibration is taken into account by assuming that it lies in line with the O-H bond. The parameters in the potential function are adjusted such that they produce the vibrational frequencies of HDO, H_2O, and D_2O.

II. RECENT EXPERIMENTAL RESULTS

Several experiments shed light on the nature of the intermolecular as well as intramolecular motions and hence on the structure of liquid water. Among these mention may be made of infrared absorption, infrared reflection, hyper-Raman scattering, inelastic neutron scattering, X-ray diffraction, and Raman scattering. Some of the useful recent results will now be discussed.

Originally, the motivation for the present work came from the report of the Raman spectral studies of HDO in H_2O by Walrafen [6] and the infrared transmittance studies of Falk and Ford [7]. Figs. 1-3, taken from Falk and Ford's paper, show the nature of transmittance as a function of frequency at a high and a low temperature. We know, that water has three fundamental vibrational bands. One of the main advantages of the study of HDO over that of H_2O or D_2O is that in HDO the three fundamentals and many of the overtone and combination bands are widely separated and thus preclude the possibility of Fermi resonance.

Figs. 4 and 5 show the photoelectric Raman spectra obtained by use of 4880-A° argon-ion-laser excitation for a 6.2 M solution of D_2O in H_2O at 25°±1°C. The OD stretching contours [8] occurring within the frequency region of 2100-2900 cm^{-1} are seen to be markedly asymmetric. The frequency of the OD stretching contour corresponding to maximum Raman intensity is 2515 ± 5 cm^{-1}. However, a pronounced high frequency shoulder is claimed [6] near 2660 ± 20 cm^{-1}.

Fig. 6 shows Raman intensities as functions of frequency transferred to horizontal baselines from mercury-excited Raman spectra of the OD stretching contour for several temperatures of 32.2 to 93.0°C. Here again marked asymmetry is evident in all of the (mercury excited) contours. Also,

FIG. 1. Compensated double-beam spectra of the stretching band, ν_3, of HDO recorded by Falk and Ford [7] at a high and a low temperature.

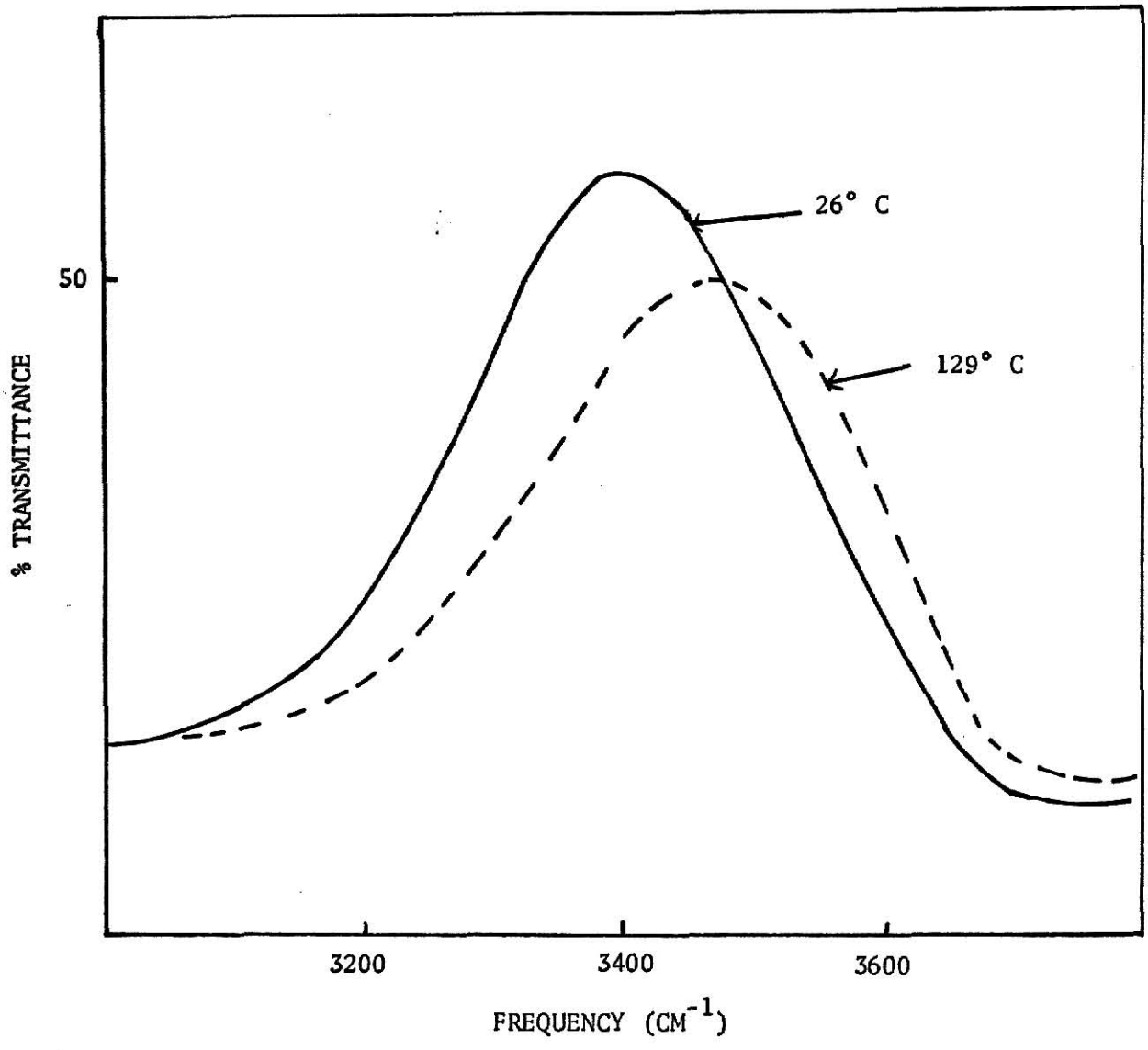

FIGURE 1

FIG. 2. Compensated double-beam spectra of the bending band, ν_2, of HDO recorded by Falk and Ford [7] at a high and a low temperature.

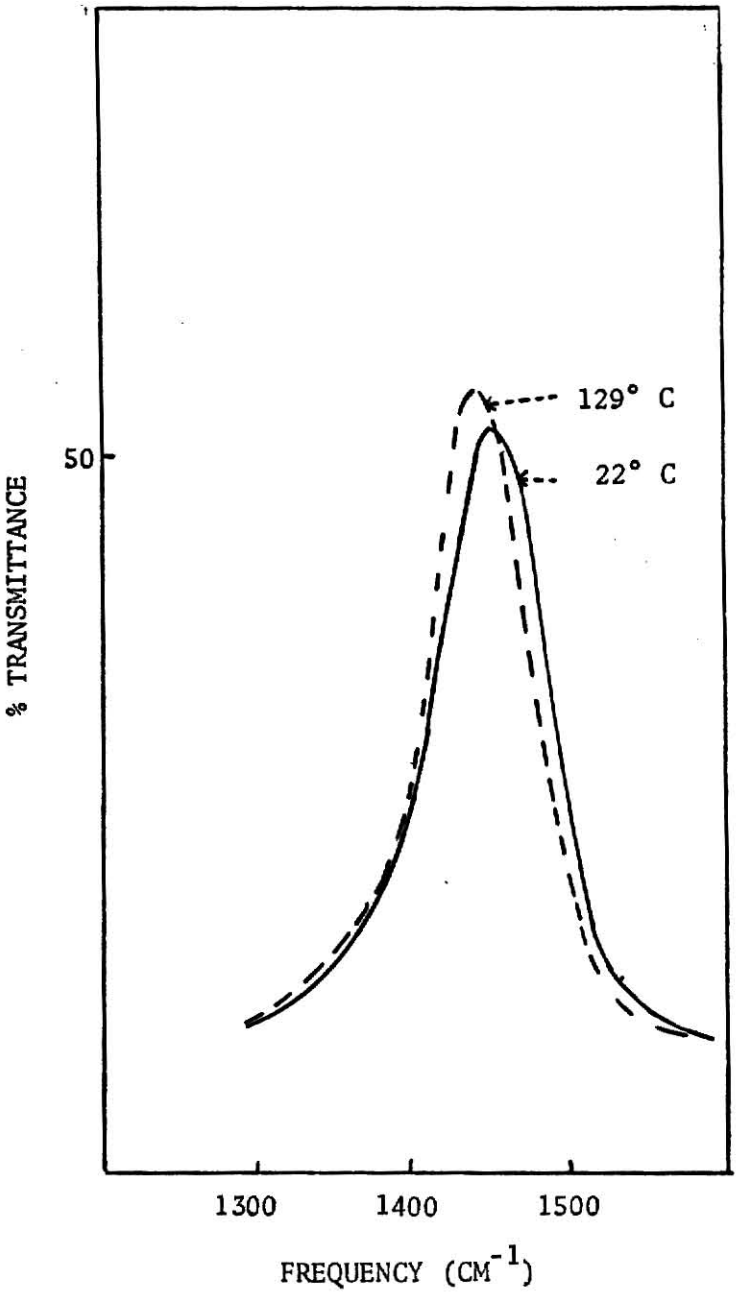

FIGURE 2

FIG. 3. Compensated double-beam spectra of the stretching band, ν_1, of HDO recorded by Falk and Ford [7] at a high and a low temperature.

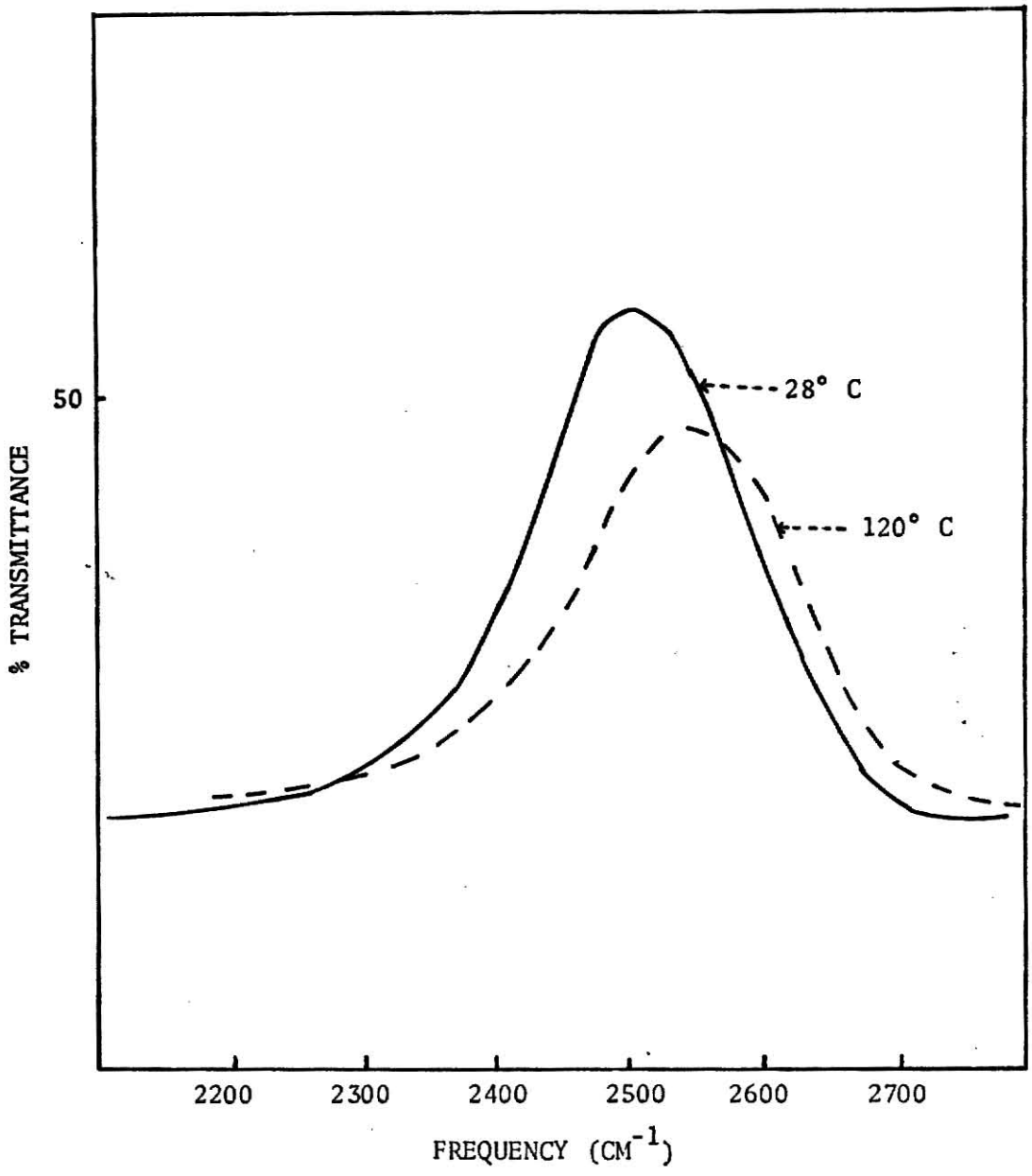
% TRANSMITTANCE
50
28° C
120° C
2200
2300
2400
2500
2600
2700
FREQUENCY (CM^{-1})

FIGURE 3

FIG. 4. Repeated Photoelectric Raman tracings from a 6.2 M solution of D_2O in H_2O at 25° C obtained with Argon-ion-laser excitation. Amplification of upper tracing is twice that of lower tracing [6].

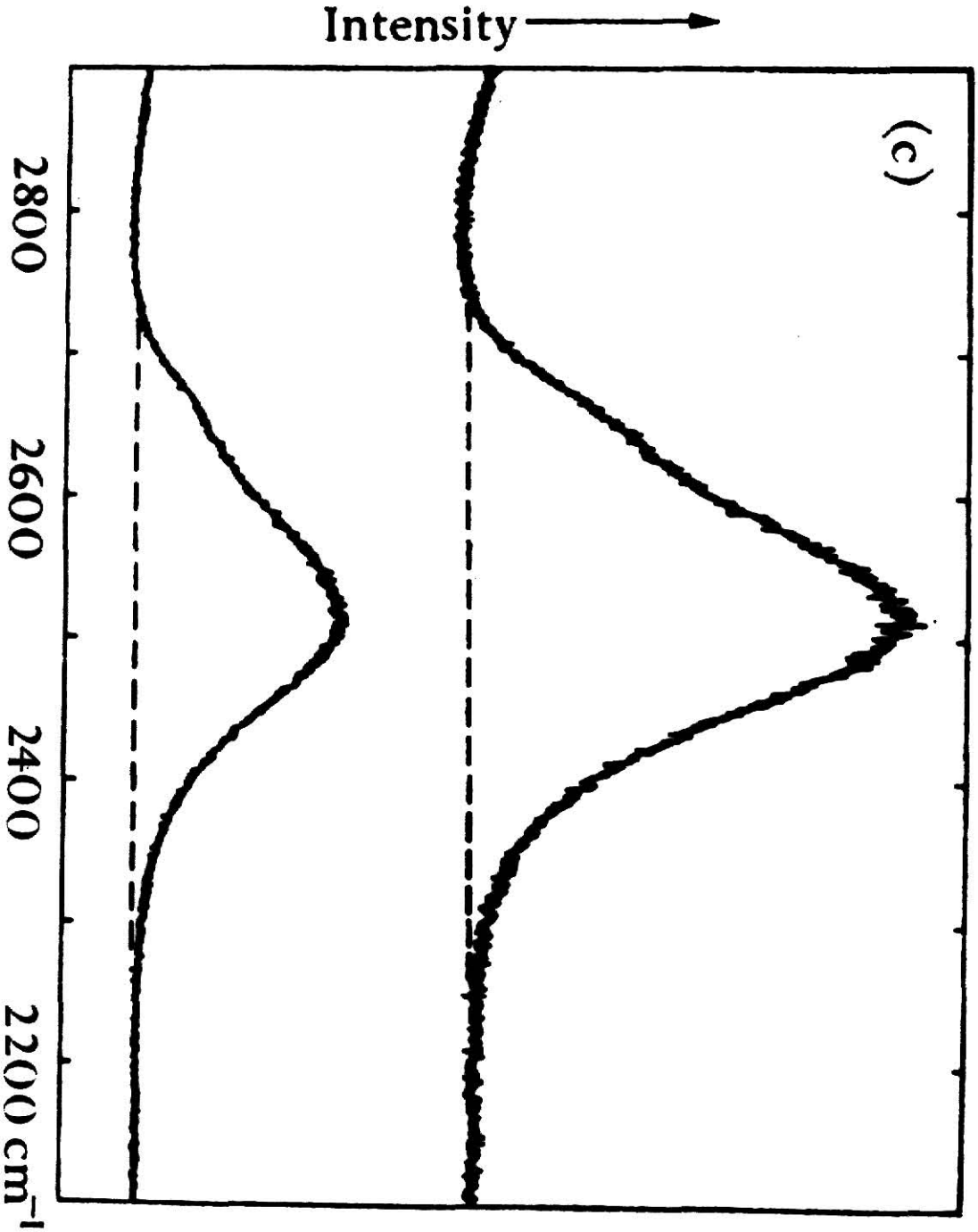

FIGURE 4

FIG. 5. Argon-ion laser Raman spectra of a 6.2 M solution of D_2O in H_2O at (25 ± 1)° C, as reported by Walrafen [6].

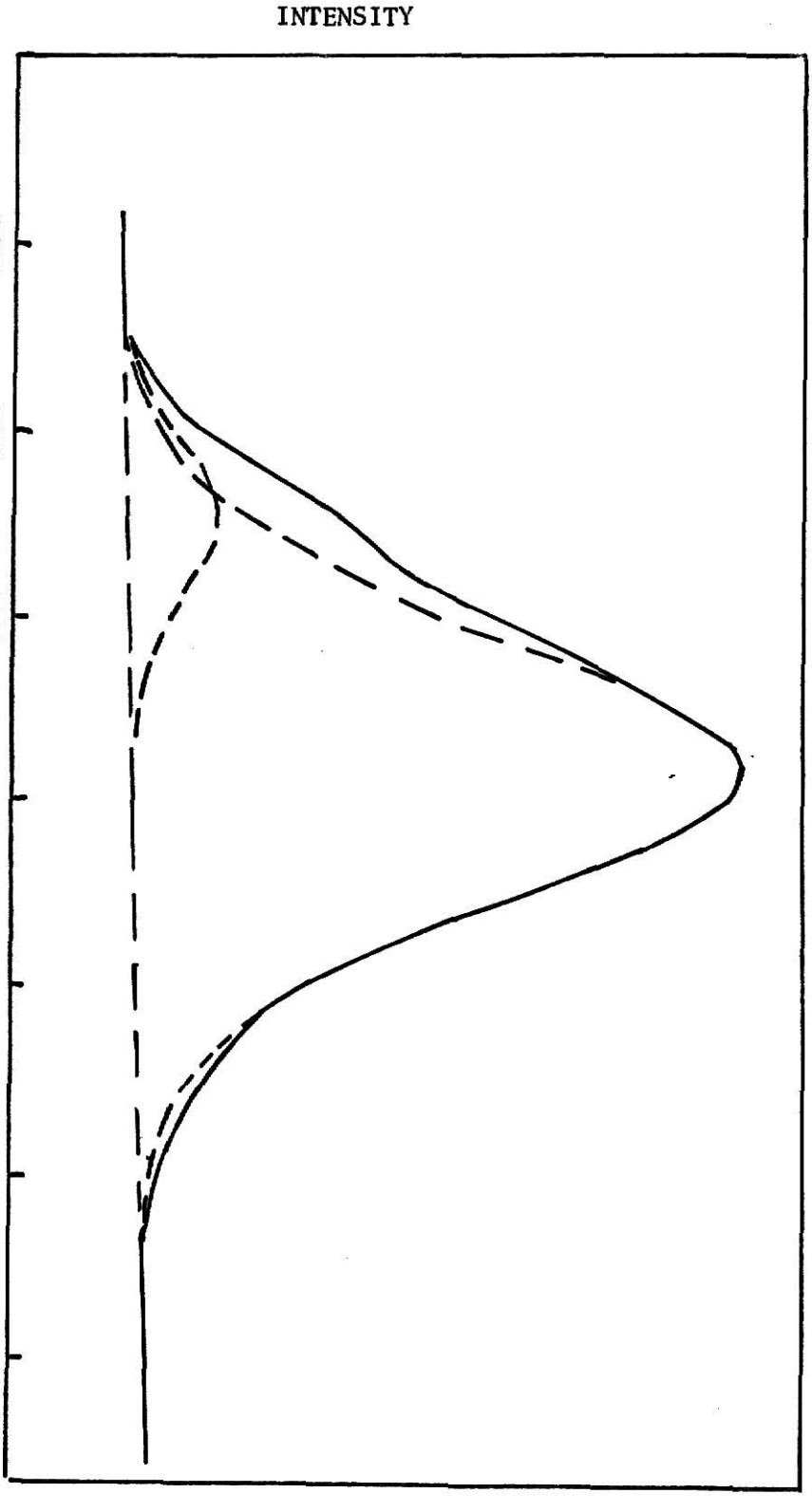

FIGURE 5

FIG. 6. Effect of temperature on the O-D uncoupled stretching band as reported by Walrafen [6]. The dashed vertical line indicates the isosbestic point near 2570 ± 10 cm^{-1}. These spectra were obtained with conventional mercury excitation and a narrow (15 cm^{-1}) slit width.

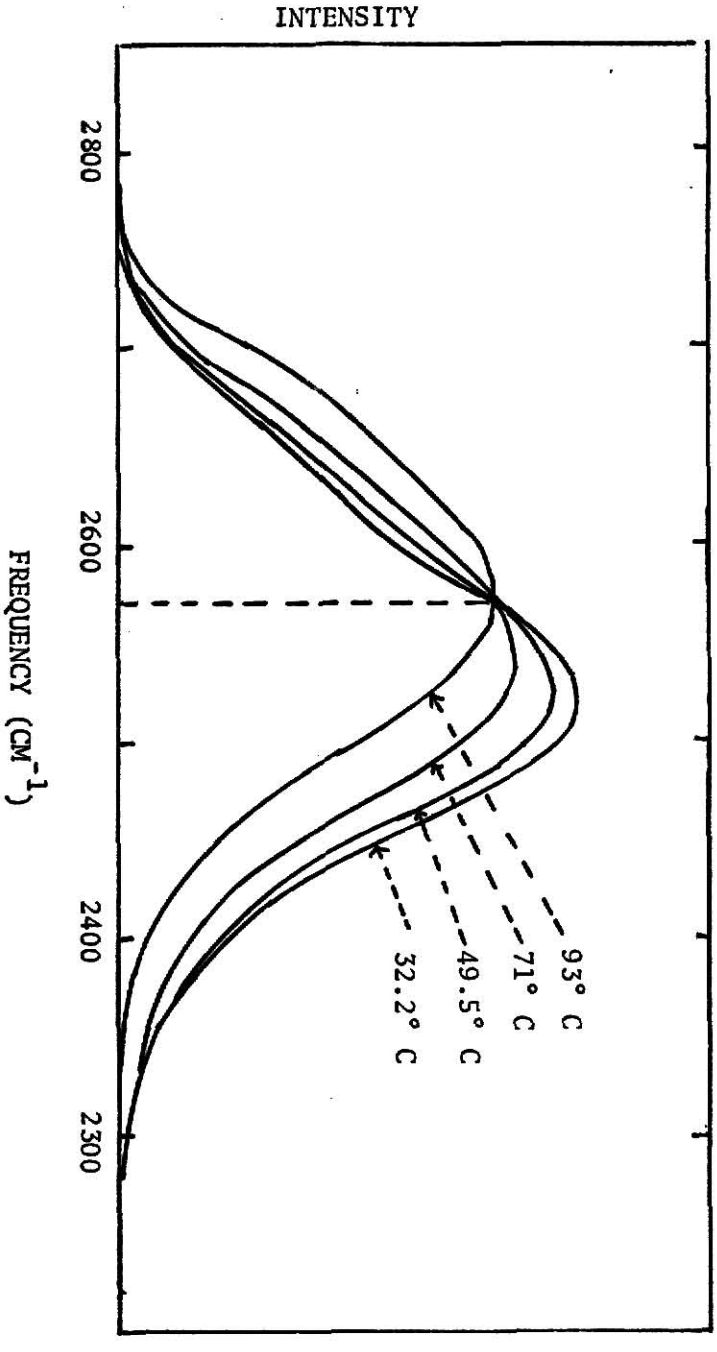
INTENSITY
2800
2600
2400
2300
FREQUENCY (CM^{-1})
93° C
71° C
49.5° C
32.2° C

FIGURE 6

these mercury-excited spectra are reported [6] to exhibit a "well defined isosbestic point" at 2570 ± 5 cm^{-1}. The total contour intensity decreases by about 17% from 32.2° to 93.0°C.

Fig. 7 shows the Raman and infrared band envelopes as reported in Wyss and Falk's paper [86].

Some of the important pieces of information about water structure come from diffraction studies. X-ray diffraction experiments have been reported by Narten, Danford, and Levy [9, 10] for water at various temperatures. From these diffraction data a radial distribution function is deduced. This function represents the average local density of molecules at a distance from the centre of an arbitrarily chosen molecule in the fluid. This function may be used for obtaining a pair correlation function, which according to Widom [106], describes the correlating effect of the presence of any one molecule on the position of a second molecule. Thus, it is a measure of the probability per unit volume of finding molecules at a distance between r and r + dr from a particular molecule. Fig. 8 shows the time correlation functions (i.e., cosine transforms), C (t), of the O-H and O-D stretching infrared bands of dilute HDO in liquid water [12]. The infrared and Raman correlation functions are generally similar in size and shape. Since this is expected only if both the experiments are looking at the same rotational-vibrational manifold, the "bumps" noted by Wall [11] in the Raman correlations are probably an artifact [12]. Infrared curves are derived from less noisy spectra.

The similarity between infrared and Raman correlation functions for HDO suggests [12] that the observed band is caused by vibrational modulation.

FIG. 7. Comparison of infrared band envelopes (Wyss and Falk [86]) with Raman band envelopes for ν_3. The dashed lines represent the infrared band envelope.

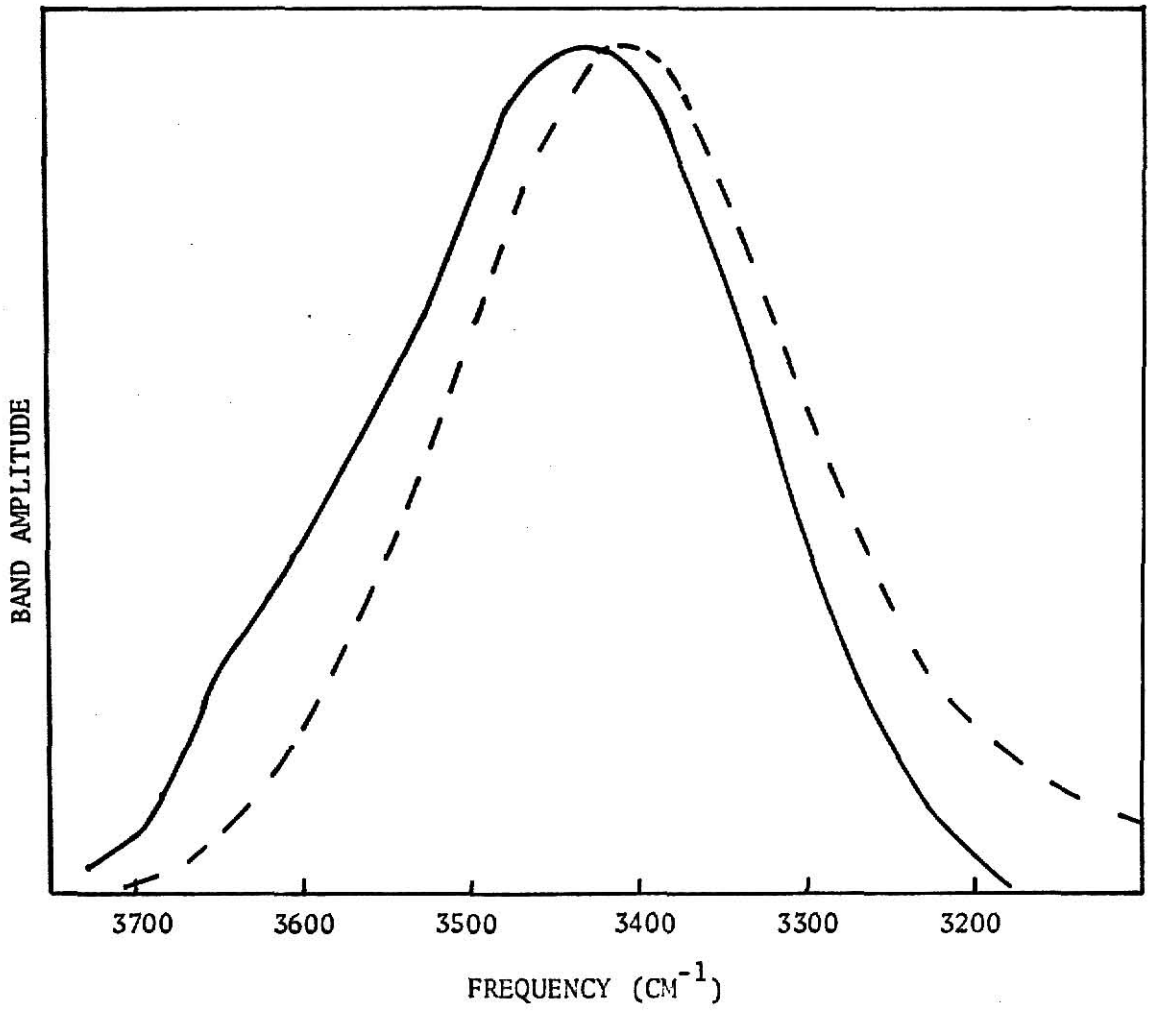

FIGURE 7

FIG. 8. Time correlation functions or cosine transforms, C(t), of the O-H (3450 cm^{-1}) and O-D (2500 cm^{-1}) stretching infrared bands of dilute HDO in liquid water. Data of 710 and 630 points, respectively, points at 10 cm^{-1} intervals. Also shown are the Raman-derived curves of Wall [11].

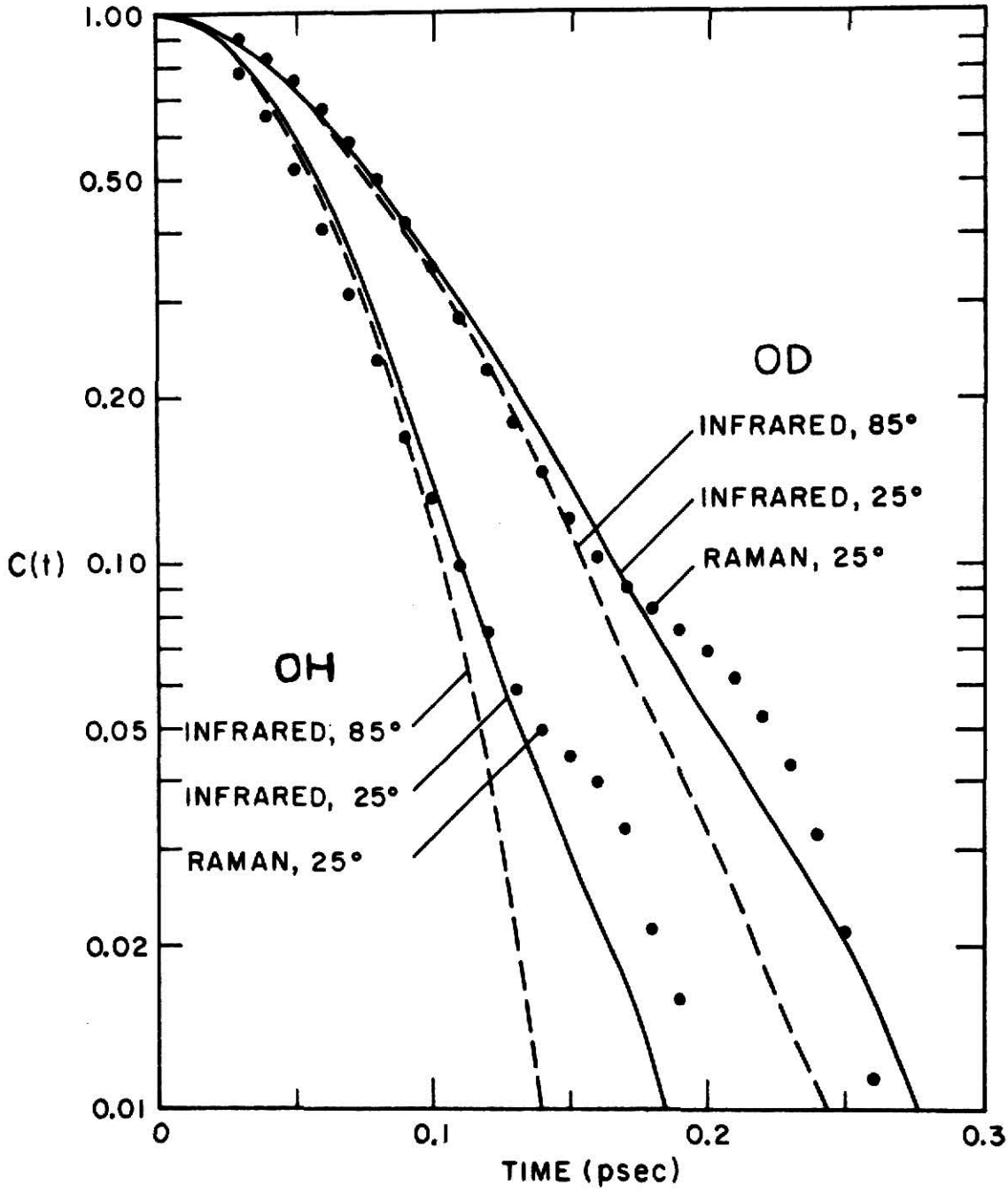
1.00
0.50
0.20
0.10
0.05
0.02
0.01
C(t)
0
0.1
0.2
0.3
TIME (psec)
OD
INFRARED, 85°
INFRARED, 25°
RAMAN, 25°
OH
INFRARED, 85°
INFRARED, 25°
RAMAN, 25°

FIGURE 8

Gordon reports [13], that, if rotational motion is responsible for an observed bandwidth, the infrared transform measures decay in the dipole transition moment vector, with cos time dependence, while the Raman transform measures scattering tensor asymmetry decay (the depolarization ratio, $\rho \lesssim 0.1$, and this is an upper limit set by analyzer polaroid leakage [42]), with $(\cos)^2$ time dependence. The observed similarity speaks strongly against broadening of the rotational band. Vibrational modulation, however, is a consequence of varying hydrogen bond strengths in liquid water [12]. Because of the highly polarized scattering, vibrational perturbations alone account for most of the breadth of the Raman band. The observed stretching bands in HDO can be envisaged as the envelope of many overlapping molecular oscillator bands, distributed densely across the observed width [12].

Thus, the rotational decay discussion of Wall [11] seems to be "naive." The temperature dependence of the infrared correlation function is consistent [12] with a bandwidth caused by vibrational perturbations and also with the simple expectation of easier rotation along with faster decay at higher temperatures.

The Raman scattering results may be summarized as follows: The Raman spectra of HDO in water show shoulders at 3640 and 2660 cm^{-1}, i.e., on the high-frequency side of the ν_3 and ν_1 bands. These shoulders, however, are not to be seen in the infrared spectra. Increasing temperature will shift the band maxima of ν_1 and ν_3 towards the high frequency side while that of ν_2 shifts toward the lower one. Also, the mercury-excited Raman spectra exhibit a "well-defined isosbestic point."

III. SOME MODELS FOR WATER

We discuss only a few of the many models proposed for water structure. Other reviews on the theories of water structure may be found elsewhere [14-27].

The common agreement for all the models proposed to date is, that they are on the whole consistent with the X-ray diffraction pattern of water. Of late, there have been formed two leading groups, one advocating the "Mixture" model while the other advocates the "Continuum" model.

The mixture models [26, 28, 29, 30-46] describe liquid water as an equilibrium mixture of molecular species with different numbers of hydrogen bonds per molecule. A species, in the terminology of Eisenberg and Kauzmann [82], is a local V-structure. In one type of mixture models two species of water molecules are supposed to be present at any given instant: molecules in clusters and monomeric, non-hydrogen-bonded molecules. The ones in clusters are hydrogen-bonded to four neighbouring molecules. At any temperature, the proportion of disruption of hydrogen bonds is well defined. Table II gives some of the estimates of the percentage of broken hydrogen bonds in water. The concentration of non-hydrogen-bonded molecules is, according to Nemethy and Scheraga's [26, 41] ideas, increased by a rise in temperature.

Mixture models have, as a special class, the interstitial models. According to these, one species of water molecule is supposed to form a hydrogen-bonded frame work containing cavities in which the other species reside [46, 49, 83].

Pople [48] has developed a model, termed the "Distorted hydrogen-bond model", and Bernal [85] has suggested a "Random network model" for the

V-Structure [82] of water. The discussion of these models is outside the scope of this thesis.

There exists very convincing evidence that the hydrogen bonds in liquid water form an extensive three-dimensional "network" [47, 50, 52]; however, this network may be short lived. The continuum models [7, 47-51, 86] hold liquid water as a complete hydrogen-bonded network. According to these, the average strength of hydrogen bonds in water is weaker than in ice because of "irregular distortion and elongation, both of which increase with temperature" [7].

While the experimental controversy has remained unsolved, it interested us to investigate the infrared and Raman spectra of liquid water from the theoretical point of view by setting up theoretical expressions for kinetic and potential energy of a general bent XYZ molecule, hydrogen bonded according to one or another of the liquid models and then solving the secular equation. This leads to the three fundamental frequencies of vibration. The probability distribution of every one of these three frequencies can then be calculated as will be shown in detail in the next chapter.

IV. THE NORMAL COORDINATE ANALYSIS

The normal coordinate analysis has been a very useful tool for describing the vibrations of a molecule. Here each atom is treated as a point mass. The force fields acting on the atoms are treated in first approximation like mechanical springs and are expressed through appropriate force constants. Thanks to the relatively simple molecular configuration and small number of vibrational models, triatomic molecules provide an encouraging field of study. Several authors [34, 53] have treated the normal modes and frequencies of vibration of the bent symmetrical XY_2 model for small vibrations. The linear symmetrical XY_2 type molecule has been treated by Adel and Dennison [57] and a linear XYZ type by Nielsen [58]. Libby [59] has studied the purely vibrational part of the problem including anharmonic terms. The bent XYZ model has been treated by Shaffer and Schuman [5] along the same lines as Shaffer and Nielson [4] for the bent XY_2 model.

The Lagrangian for a vibrating molecule is $L = T - V$, where T and V denote the kinetic and potential energies of the system. The set of equations to be solved are the Lagrange's equations of motion, viz., $\frac{d}{dt}(\frac{\partial L}{\partial \dot{q}_k}) = \frac{\partial L}{\partial q_k}$, where $\dot{q}_k$ and q_k are the generalized velocities and the displacements of the constituent atoms, respectively. Assuming the constraints to be scleronomous and the generalized coordinates not to be explicitly dependent on time and that T is a homogeneous quadratic function of the velocities, we have

$$T = \frac{1}{2} \sum_{k,i=1}^{3} \mu_{ki} \dot{q}_k \dot{q}_i$$

Similarly, the potential energy has a Taylor series expansion of the form

$$V = V_0 + \sum_{k=1}^{3} \left(\frac{\partial V}{\partial q_k}\right)_0 q_k + \frac{1}{2!} \sum_{i=1}^{3} \left(\frac{\partial^2 V}{\partial q_k \partial q_i}\right)_0 q_k q_i + \cdots$$

$$= V_0 + \sum_{k=1}^{3} V_k q_k + \frac{1}{2!} \sum_{k=1}^{3} \sum_{i=1}^{3} V_{ki} q_k q_i$$

All the $q_k = 0$ at the equilibrium position, so that $\left.\frac{\partial V}{\partial q_k}\right]_0 = 0$.

That is, $\underline{F} = -\underline{\nabla} V = \underline{0}$, at equilibrium. Since the choice of the zero of potential energy is arbitrary, the V_0 term can be chosen so that $V = 0$ at the equilibrium position. Thus,

$$V = \frac{1}{2!} \sum_{k=1}^{3} \sum_{i=1}^{3} V_{ki} q_k q_i + \cdots$$

$$T = \frac{1}{2!} \sum_{k=1}^{3} \sum_{i=1}^{3} \mu_{ki} \dot{q}_k \dot{q}_i + \cdots = \frac{1}{2!} \sum_{k=1}^{3} \sum_{i=1}^{3} T_{ki} \dot{q}_k \dot{q}_i + \cdots$$

The Langrange's equations of motion are

$$\frac{d}{dt}\left(\frac{\partial L}{\partial \dot{q}_k}\right) = \frac{\partial L}{\partial q_k} = \frac{d}{dt}\left\{\sum_{i=1}^{3} \mu_{ik} \dot{q}_i\right\}$$

and form a system of coupled nonlinear second order differential equations. Differentiation and linearization of the system yields

$$\sum_{j=1}^{3} T_{ji} \ddot{q}_j = -\sum_{k=1}^{3} V_{ki} q_k .$$

This truncation of the Taylor series is justified only by the smallness of vibrations, since the higher order terms become important only for large displacements. This truncation gives $T\{\ddot{q}\} = -V\{q\}$. V and T are symmetric matrices, not necessarily diagonal. A matrix R is chosen such that $R'TR = I$, where R' is the transpose of R, and I is the identity matrix (see Appendix III for details). If $R'VR = A$, the above equation becomes $\{\ddot{q}\} = -A\{q\}$.

Seeking a periodic solution of the form $\{q^{(t)}\} = \{q^{(o)}\}e^{i\omega t}$, we get

$$\omega^2 \{q^{(o)}\}e^{i\omega t} = A\{q^{(o)}\}e^{i\omega t}$$

If we multiply by $e^{-i\omega t}$, the eigenvalue equation becomes

$$A\{q^{(o)}\} = \omega^2 \{q^{(o)}\}.$$

Thus, when we diagonalize A, we get ω_1^2, ω_2^2, ω_3^2.

The secular equation problem was solved on a computer using a diagonalization procedure due to Jacobi [65]. The Jacobi method annihilates step by step the off diagonal elements of A by performing generalized coordinate rotations. It is an iterative scheme and converges to the diagonalized matrix to a specified degree of accuracy. The results give both the eigenvalues and the eigenvectors. As is shown in the outline of the program the eigenvectors are normalized to unity (cf. Appendix IV). Bryan [66] has indicated that the small oscillations treatment may be used with justification.

Our treatment differs a little from that of Shaffer and Schuman [5] in that we have taken the OD and OH distances to be different, and hence that $k_o \neq l_o$. That is, we have relaxed the assumption that HDO has the same equilibrium configuration as H_2O and D_2O. The kinetic energy of vibration of bent XYZ molecule is (cf. Appendix II for definitions of coordinates and algebraic details)

$$2T = [\mu_{11}\dot{u}^2 + \mu_{22}\dot{v}^2 + \mu_{33}\dot{w}^2 + 2\mu_{12}\dot{u}\dot{v} + 2\mu_{23}\dot{v}\dot{w} + 2\mu_{13}\dot{u}\dot{w}].$$

The harmonic potential energy function is

$$2V = [C_{12}r_2'^2 + C_{13}r_3'^2 + C_2\beta'^2 + 2C_3\beta'(r_2' + r_3') + 2C_4 r_2' r_3']$$

$$= k_{11}u^2 + k_{22}v^2 + k_{33}w^2 + 2k_{12}uv + 2k_{23}vw + 2k_{13}uw$$

where

$$k_{ij} = \{(A_i A_j) C_{12} + (B_i B_j) C_{13} + C_i C_j C_2 + [(A_i + B_i) C_j + (A_j + B_j) C_i] \times C_3 + (A_i B_j + B_i A_j) C_4\}$$

The force constants, C's, were chosen as follows: To start with, C_{12} and C_{13} were taken to be the same and called k_H. Varshni [61], has made a comparative study of most of the potential energy functions for diatomic molecules. He reports that the Lippincott-Schroeder equation gives the most accurate value of $\omega_e x_e$. We have chosen the k_H value from Lippincott and Schroeder's paper [62, 63]. In particular, in the equation

$$k_H = \left(\frac{nD}{r^3}\right)\left[\exp\left(-\frac{n\Delta r^2}{2r}\right)\right]\left[r_0^2 - \frac{n(\Delta r)^2}{4r}(r+r_0)^2\right] + \left\{\frac{n^* D^*}{(R-r)^3}\exp\left[-\frac{n^*(R-r-r^*)}{2(R-r)}\right]\right\}\left[r_0^{*2} - n^*(R-r-r_0^*)^2\frac{(R-r+r_0^*)^2}{4(R-r)}\right],$$

we put

$$r_0 = r = 0.97 \times 10^{-8}\ cm, \quad n = 9.18 \times 10^8\ cm^{-1},$$

and set $nD = k_0 r_0 = n^* D^*$ This gives $D = 0.8199 \times 10^{-11}\ kcal./mole,$

and $n^* = 13.32 \times 10^8\ cm^{-1}$

The value of k_H obtained by setting $R = \infty$ and $\Delta r = r - r_0 = 0$ is, $k_H = 7.7213 \times 10^5\ dynes\ cm^{-1}$

The constant k_H determined by setting R = ∞ implies that it is an equilibrium constant determined in absence of the effects of neighbouring oxygen atoms, and is thus the O-H stretching force constant for an isolated (vapour) water molecule. The fixing of the constants C_1, C_2, C_3 and C_4 was by and large a trial and error procedure. Help was sought of equations

II-109 through II-118 of Herzberg [64], and from the articles listed in References 56, 76, 84, 87, 88, and 90. The resulting force constant values, adjusted so as to conform with the form of the potential energy function and in agreement with the infrared and Raman frequency maxima for liquid water, are:

$$k_H = 7.7213 \times 10^5 \text{ dcm}^{-1}$$
$$C_2 = 0.2019 \times 10^6 \quad "$$
$$C_3 = 0.3877 \times 10^5 \quad "$$
$$C_4 = -0.0794 \times 10^5 \quad "$$

Since the centre of mass of the whole molecule is very close to the O atom and since the contributions from the rotational molecular motions involve mostly H atoms, the contributions from the rotational molecular motions were omitted. The X-rays do not scatter appreciably from the H atoms having a single electron so that the pair correlation function measures predominantly the position correlations of an "oxygen lattice." For translational motions the O atoms are displaced more and therefore their translations were assumed to contribute to the pair correlation function.

From the work of Narten, Danford, and Levy [9], a pair correlation function may be obtained. Fig. 9 shows a portion of the pair correlation curve represented by open circles. The first maximum at an O-O distance of about 2.85 A° represents the contribution of the nearest neighbours. The upper limit of the nearest neighbour distribution was arbitrarily fixed by a straight line drawn tangent to the curve at the inflection point slightly to the right of the first maximum of the pair correlation function. The area enclosed by the line through the open circles and bounded by the straight tangent line was assumed to represent the distribution of nearest neighbour

FIG. 9. The pair correlation function for liquid water at 25° C vs. the O-O distance is denoted by circles. The nearest neighbor contribution was assumed to be represented by the skewed Gaussian-shaped curve. This was obtained from the work of Narten, Danford, and Levy [9].

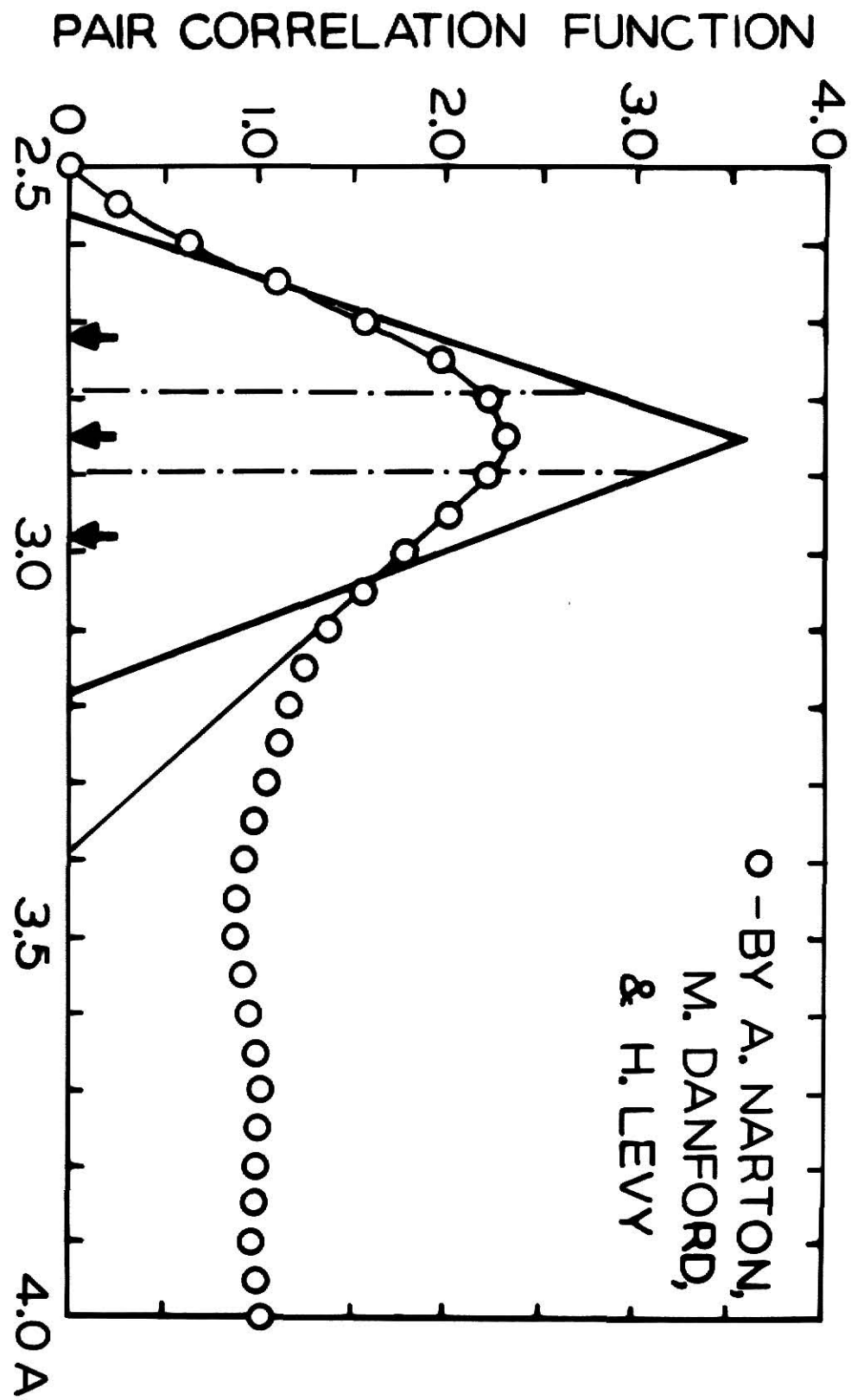
PAIR CORRELATION FUNCTION
0
1.0
2.0
3.0
4.0
2.5
3.0
3.5
4.0 A
O-O DISTANCE
O-BY A. NARTON,
M. DANFORD,
& H. LEVY

FIGURE 9

O-O distances including vibrations. The approximate unfolding of the vibrations was accomplished as follows: The classical turning points were matched with upper and lower limits of the nearest neighbour distribution. These were computed using the potential function of Lippincott and Schroeder [62, 63], and are shown in the Figs. 9 and 10. This gave the corresponding upper (RFLMX) and lower (RFLMN) equilibrium distances. The O-O equilibrium distance distribution was then approximated by a triangle peaked at the maximum (RFLCR) of the pair correlation function curve and passing through these points. The area of this triangle was chosen to be equal to the area representing the nearest neighbours including vibrations and is called here the corrected nearest neighbour pair correlation function. Later this distribution was used as the basis for a monte carlo calculation.

The X-ray diffraction experiments give evidence that there is a distribution of O-O distances in liquid water. The Lippincott and Schroeder potential function indicates that the strength of the hydrogen bond varies rapidly with this O-O distance. This implies that there is a distribution of vibrational frequencies in liquid water. This distribution of frequencies was calculated using the following procedure: The RFLMN, RFLMX and RFLCR in the computational program were determined from X-ray data [9, 66]. The range (RFLMX-RFLMN) was divided into one hundred equal parts. By assigning the hydrogen bonds random lengths the corresponding values of the O-O distance, RFL, and O-H force constant, k_H, were determined. These lengths were chosen by selecting two two-digit random numbers generated with the help of a computer. The set of random numbers generated has been tested by Dhingra [79] by frequency test and serial test and the numbers have been found to be random to the 95% confidence level. Each two digit number represents a

FIG. 10. Potential energy curves for a hydrogen bond at three equilibrium distances are shown as a function of O-O distance. The solid curves were calculated from the Lippincott and Schroeder potential function. The dotted curves are those published by Lippincott and Schroeder [62, 63].

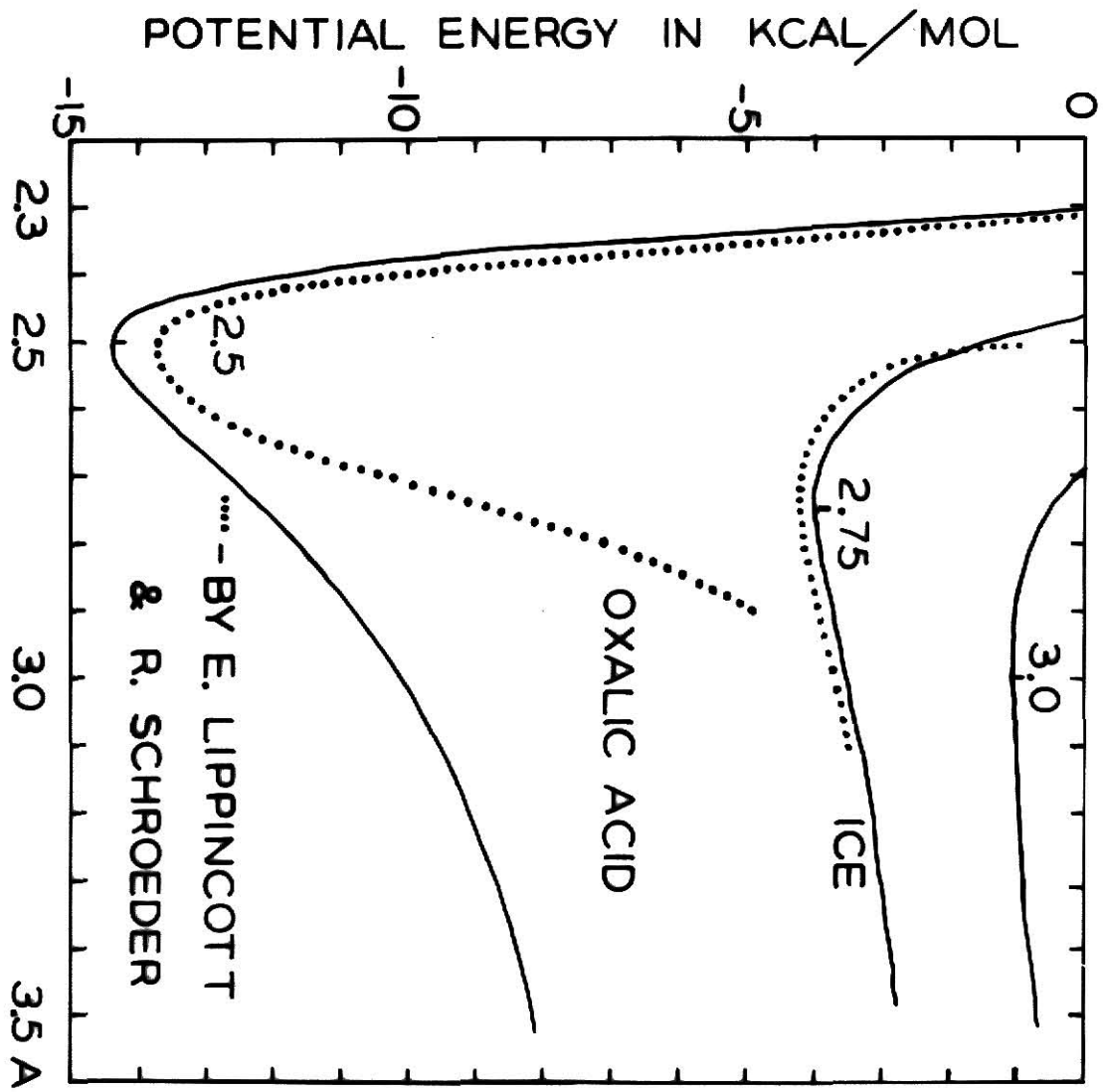
POTENTIAL ENERGY IN KCAL/MOL
0
-5
-10
-15
2.3
2.5
3.0
3.5 A
O-O DISTANCE
2.5
2.75
3.0
ICE
OXALIC ACID
---- - BY E. LIPPINCOTT
& R. SCHROEDER

FIGURE 10

particular O-O distance. The height of the corrected nearest neighbor pair correlation function represents the probability that an O-H....O bond has the corresponding O-O length at equilibrium. The hydrogen bond lengths in a configuration with two hydrogen bonds are assumed to be all independent and hence the product of the two separate O-O length probabilities gives the probability of finding that particular configuration. From the O-O distance, the appropriate force constants were evaluated. This random number sampling technique was preferred since the consideration of all 100 configurations would require $(10^2)^2 = 10^4$ calculations to cover the entire population of possible configurations. The frequency was analyzed in steps of 15 cm^{-1}.

An example of one calculation will be outlined here in order to indicate the procedure more clearly. This represents a single configuration in the random number procedure. Assume that two sets of random digits 65 and 71 are generated. These specify the two boxes corresponding to O-O distances RFL (65) and RFL (71) in the O-O distance distribution. The height of the corrected nearest neighbor pair correlation function represents the relative probability, H (RFL), for an O-O bond, having that particular length RFL (i). The relative probability of the configuration is PHT = H(65) H(71). Corresponding O-H distances R(i) and the associated k_H values are automatically determined through the Lippincott and Schroeder potential function (see the computer program, Appendix IV). Thus, the set of random digits determines values for k_H (65), k_H (71), RFL (65), RFL (71), R(65), R(71), H (65), and H (71). These, along with other geometrical and mass constants, serve as input parameters which determine the elements in the (3X3) matrix A, which is then diagonalized. The eigenvalues obtained from the diagonalization, λ_1, λ_2, and λ_3, are related to the frequencies in cm^{-1} by the relationship,

$\nu_i = (\frac{1}{2\pi c})(\lambda_i)^{1/2}$, where c is the speed of light. The results from the Random number calculations yield the frequency distributions shown in Figs. 11-17.

FIG. 11. A histogram of frequency distribution for the stretching band, ν_3, at 25° C.

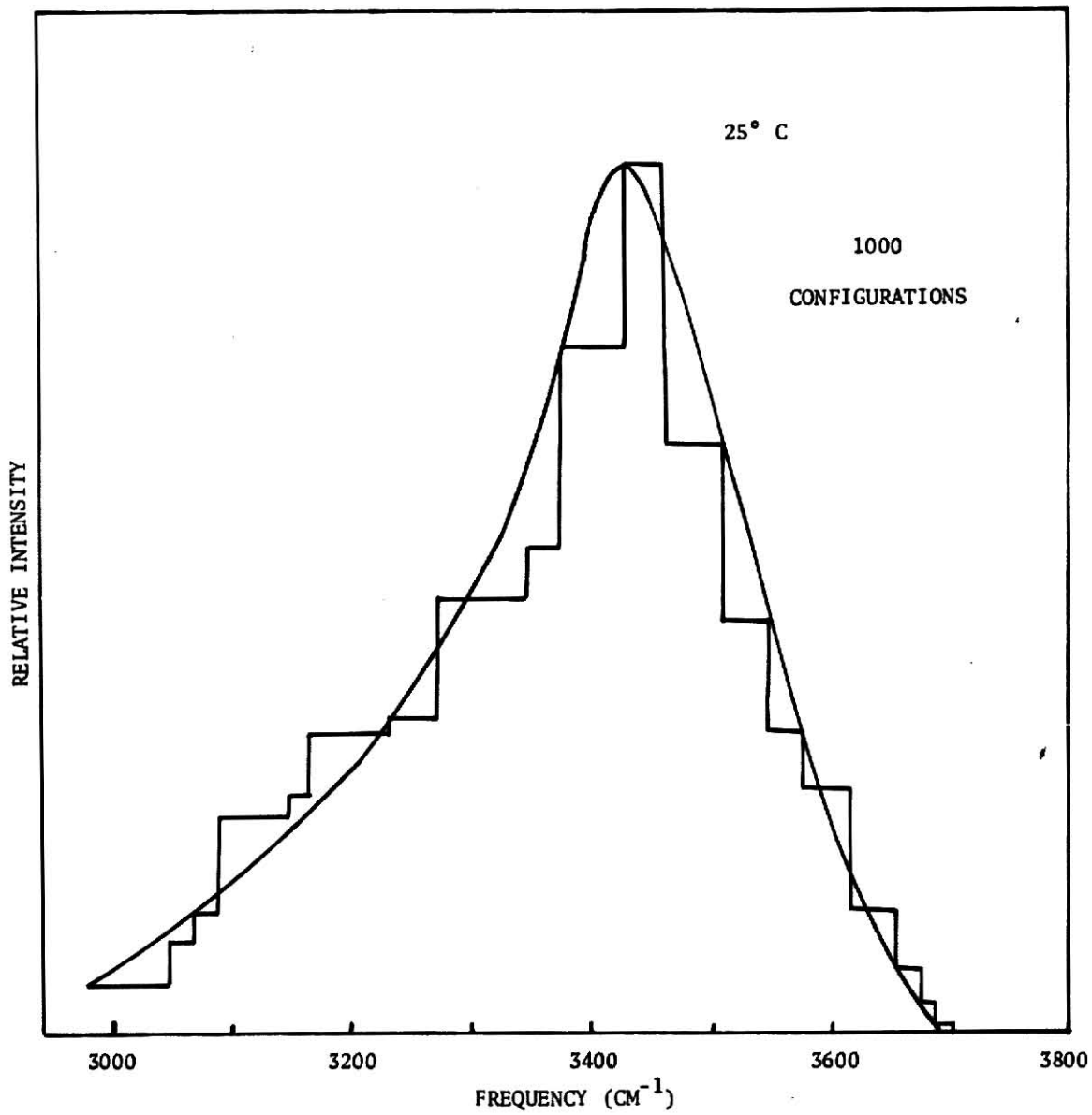
25° C
1000
CONFIGURATIONS
RELATIVE INTENSITY
3000
3200
3400
3600
3800
FREQUENCY (CM^{-1})

FIGURE 11

FIG. 12. Theoretical frequency distribution for the stretching band, ν_3, as a function of temperature.

These curves and the remainder of the results presented represent a smooth curve drawn through a computed histogram as in Fig. 11 and may be considered to be uncertain in abscissa to ± 20 cm^{-1}.

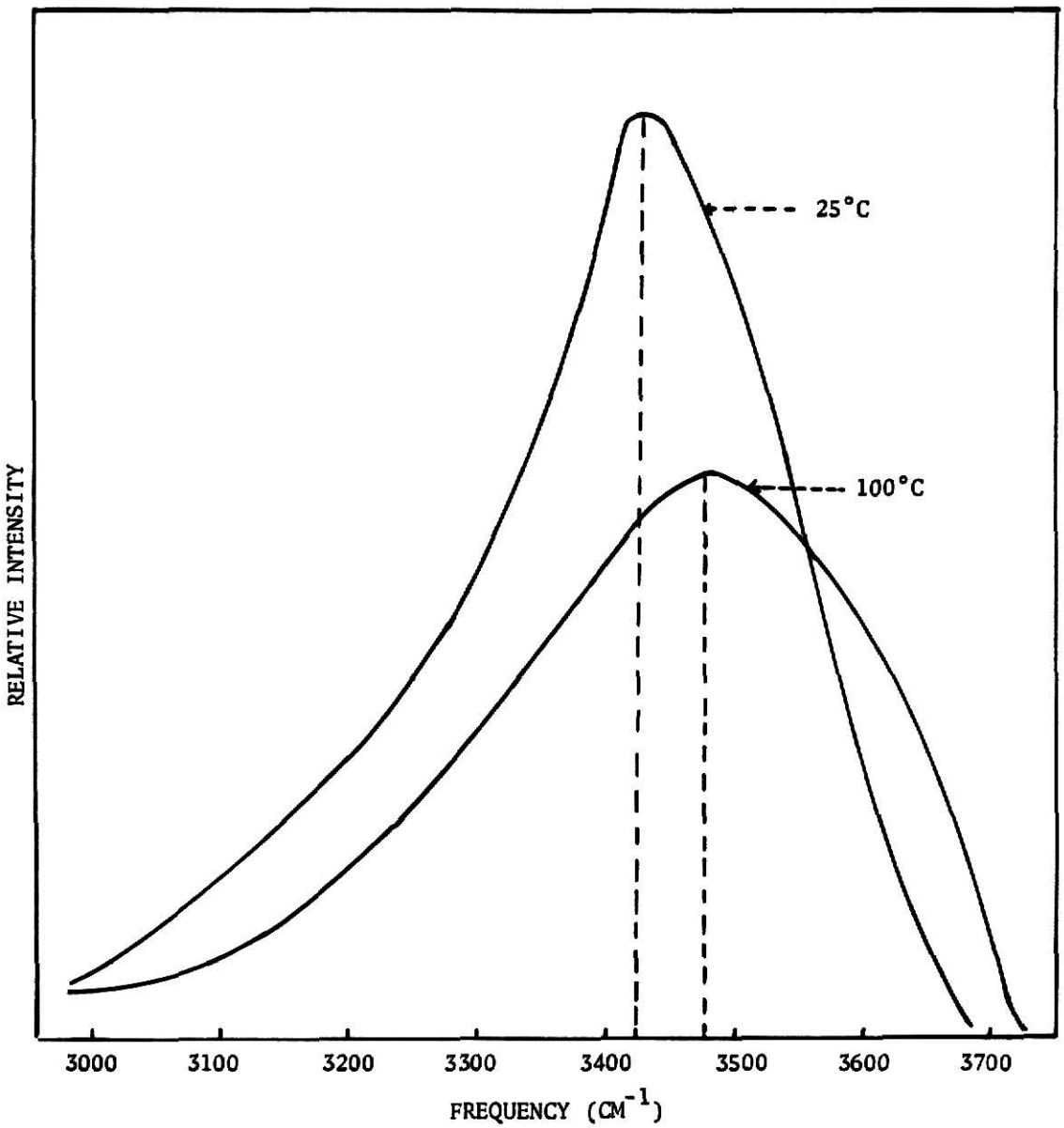
25°C
100°C
RELATIVE INTENSITY
3000
3100
3200
3300
3400
3500
3600
3700
FREQUENCY (CM^{-1})

FIGURE 12

FIG. 13. Theoretical frequency distribution for the stretching band, ν_1, as a function of temperature.

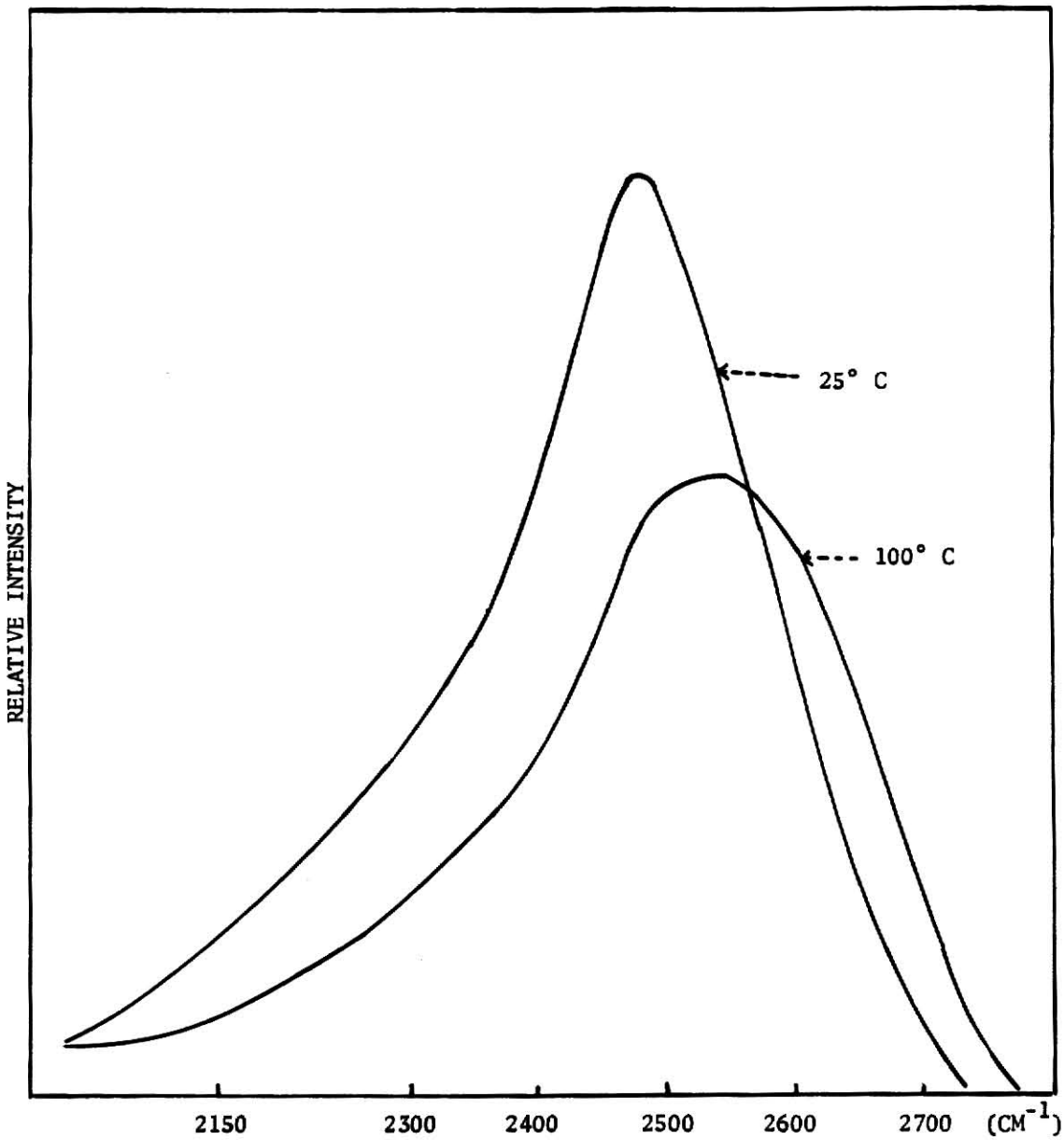
RELATIVE INTENSITY
25° C
100° C
2150
2300
2400
2500
2600
2700
(CM^{-1})

FIGURE 13

FIG. 14. Theoretical frequency distribution for the bending band, ν_2, as a function of temperature.

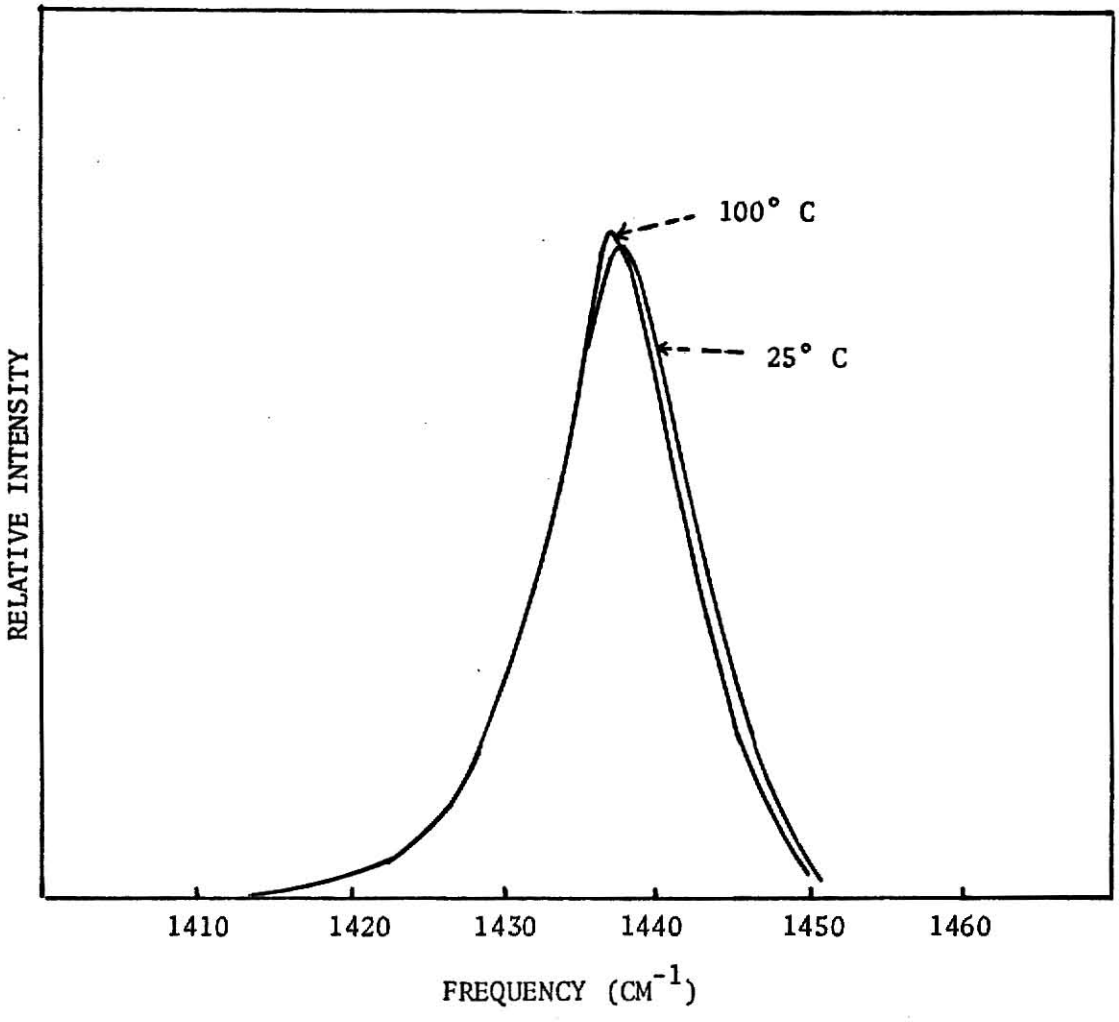
100° C
25° C
RELATIVE INTENSITY
1410
1420
1430
1440
1450
1460
FREQUENCY (CM^{-1})

FIGURE 14

FIG. 15. Effect of temperature on the O-D uncoupled stretching band, ν_1, as given by this theory. The isosbestic point is at 2560 ± 15 cm^{-1}.

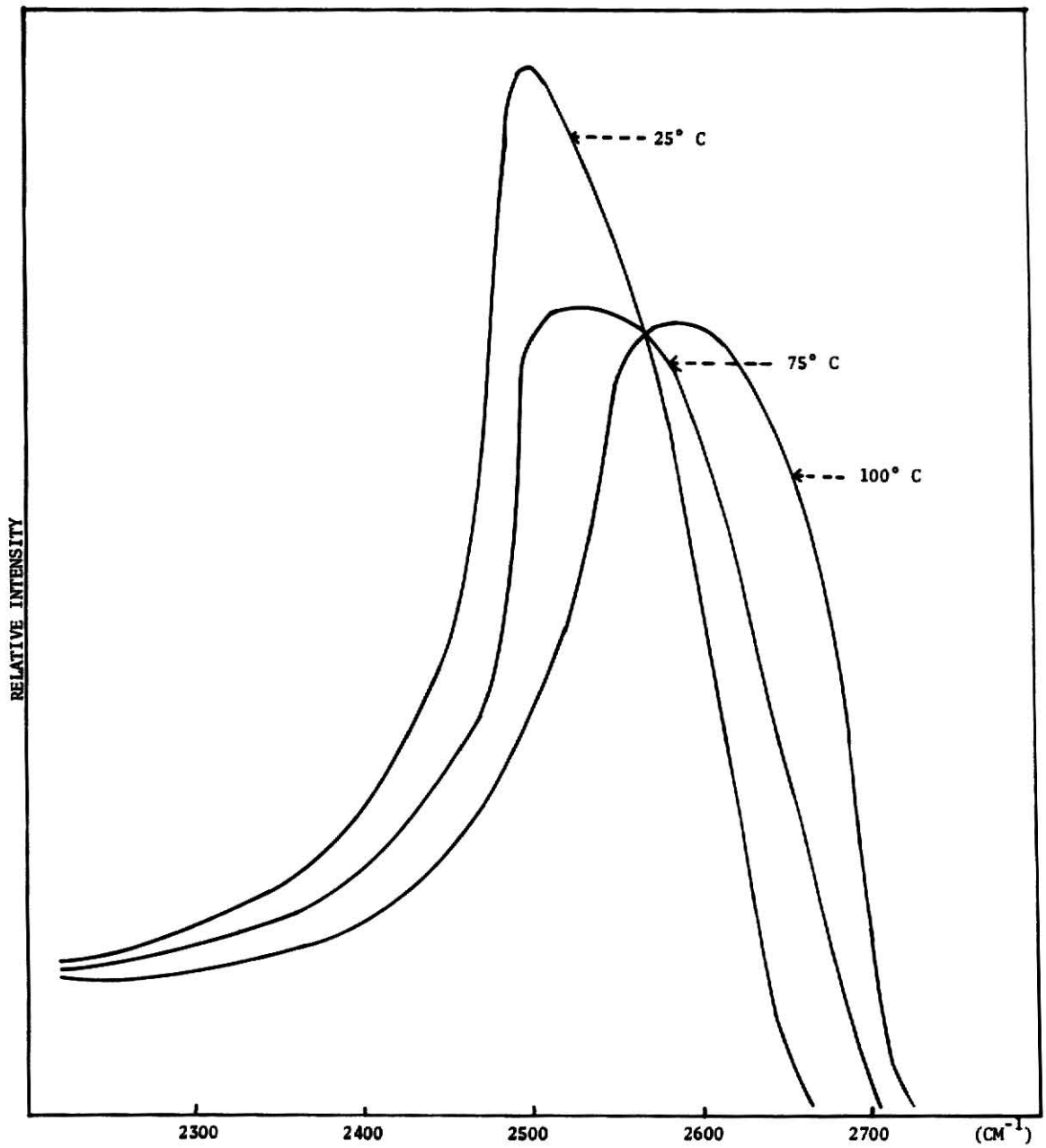
25° C
75° C
100° C
RELATIVE INTENSITY
2300
2400
2500
2600
2700
(CM⁻¹)

FIGURE 15

FIG. 16. Comparison of theoretical and experimental curves for the stretching band, ν_3. The experimental curve is due to Wyss and Falk [86].

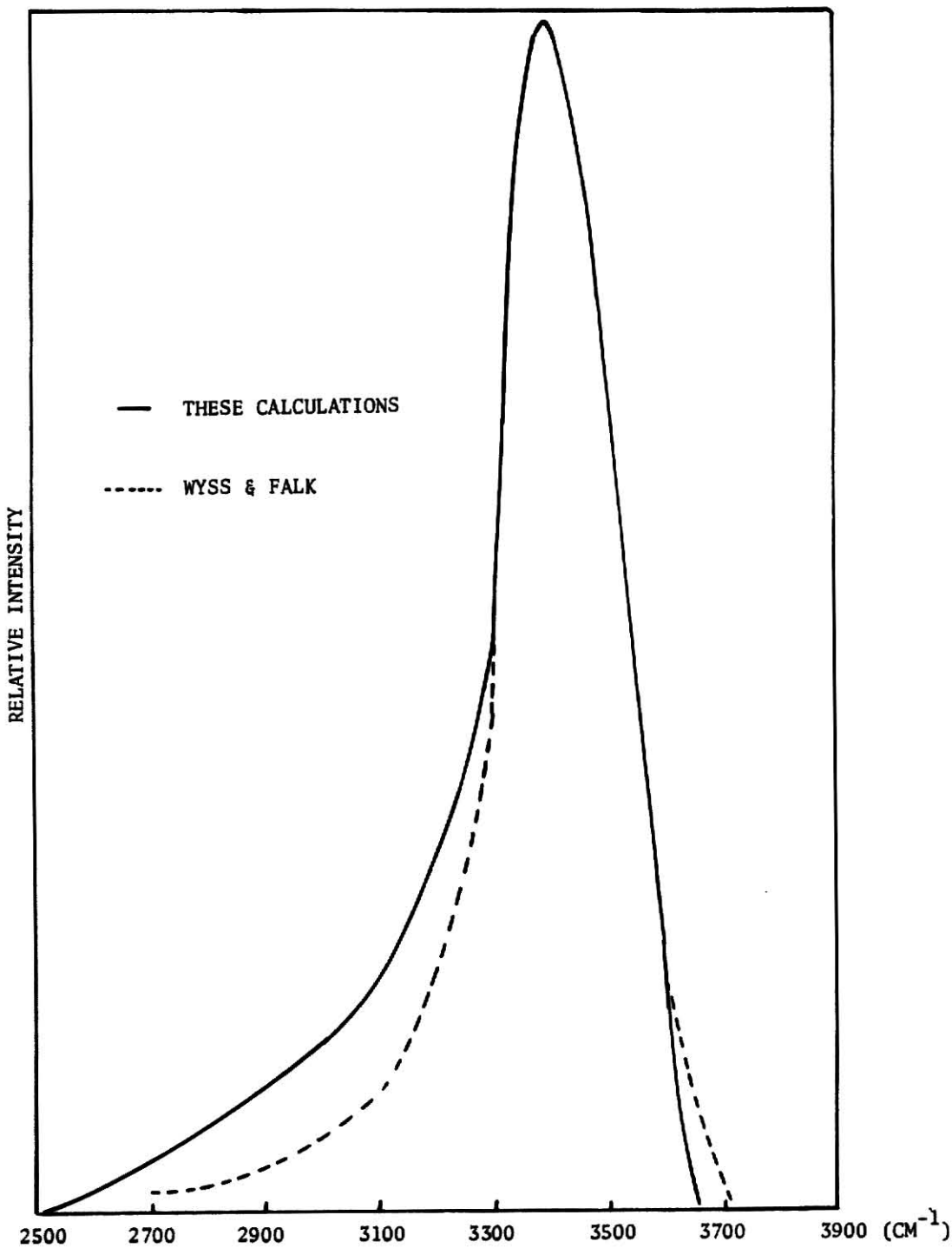
THESE CALCULATIONS
WYSS & FALK
RELATIVE INTENSITY
2500
2700
2900
3100
3300
3500
3700
3900
(CM-1)

FIGURE 16

FIG. 17. Comparison of theoretical and experimental curves for the stretch-band, ν_1. The experimental curve is due to Walrafen [6].

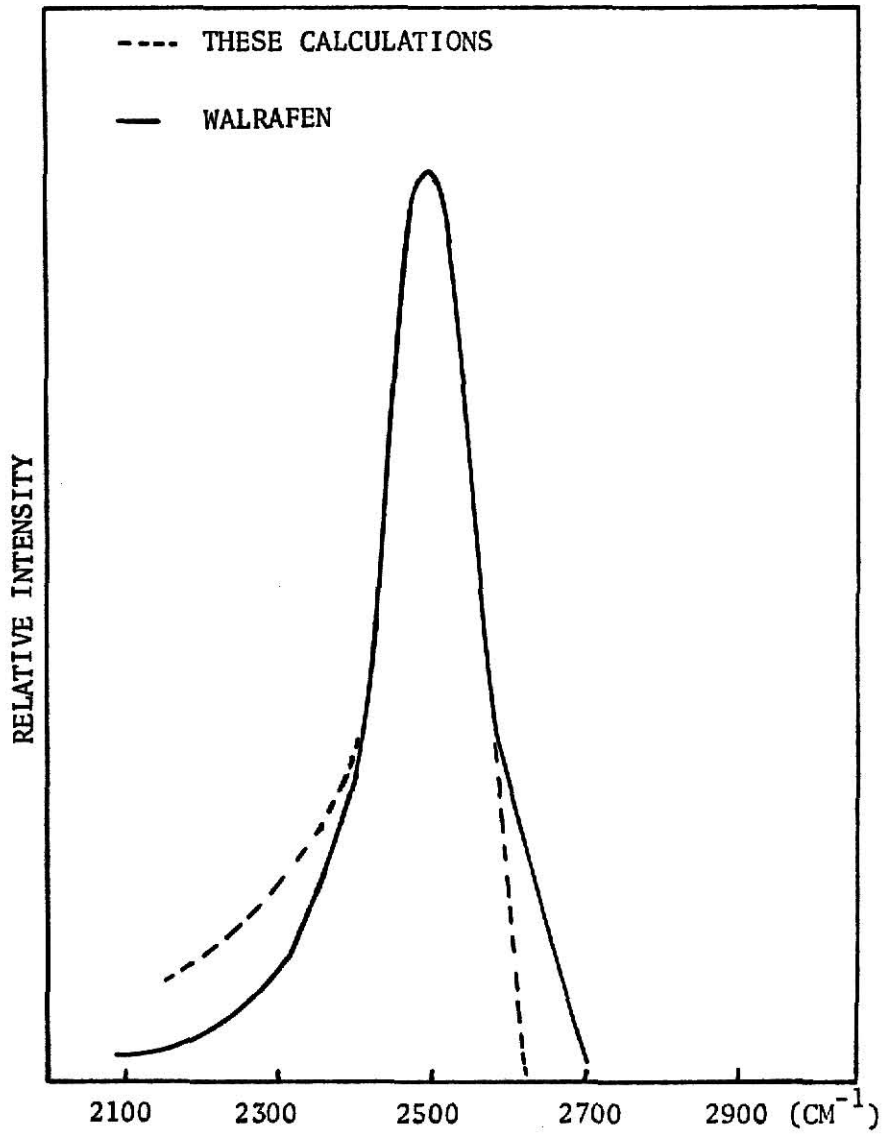
---- THESE CALCULATIONS
— WALRAFEN
RELATIVE INTENSITY
2100
2300
2500
2700
2900 (CM^{-1})

FIGURE 17

V. DISCUSSION

On the Choice between Mixture and Continuum Models:

A look at the Figures 5, 7, and 18 shows that each of the fundamental bands of HDO shows a single maximum with ν_3 and ν_1 having shoulders in the Raman Spectra at 3640 ± 10 cm^{-1}, and 2560 ± 10 cm^{-1}, respectively. Increase of temperature causes a uniform shift of the whole band, being to higher frequencies for the stretching modes of vibration, ν_3 and ν_1, and toward lower frequencies for the bending mode, ν_2. The half-widths of ν_3, ν_1, and ν_2, are 255 ± 10, 170 ± 10, and 12 ± 3 cm^{-1}, respectively, and are almost constant at all temperatures. We have no way of accounting for the variation of the bending constant with O-O distance so as to lead to the observed half-width for ν_2 and have not attempted to treat this feature of the spectrum. The transmittance of ν_3 and ν_1 increases with temperature while that of ν_2 shows a decrease. These are the conclusions reached on the basis of a far simpler Continuum Model and these have been experimentally verified [6, 7, 86] except for ν_2.

The shoulders in the Raman Spectra appear to have a simple explanation in terms of the Continuum Model. The potential function used, being anharmonic in nature, carried with it our anticipatory guess that the shoulders might be the manifestations of the overtones of the hindered translational band, ν_T, observed in H_2O at 193 cm^{-1} at 30°C [104]. Computations with a modified computer program revealed that the position of the peak and the half-width of the shoulder agree within experimental errors with the observed values. Since no a priori way of handling the relative intensities of the fundamental and the corresponding overtone bands was in sight, only the occurrence of overtones at different temperatures is predicted in Table I.

FIG. 18. Comparison of infrared band envelopes (Wyss and Falk [86]) with Raman band envelopes (Walrafen [6]) for ν_1. Infrared band is indicated by dashed lines.

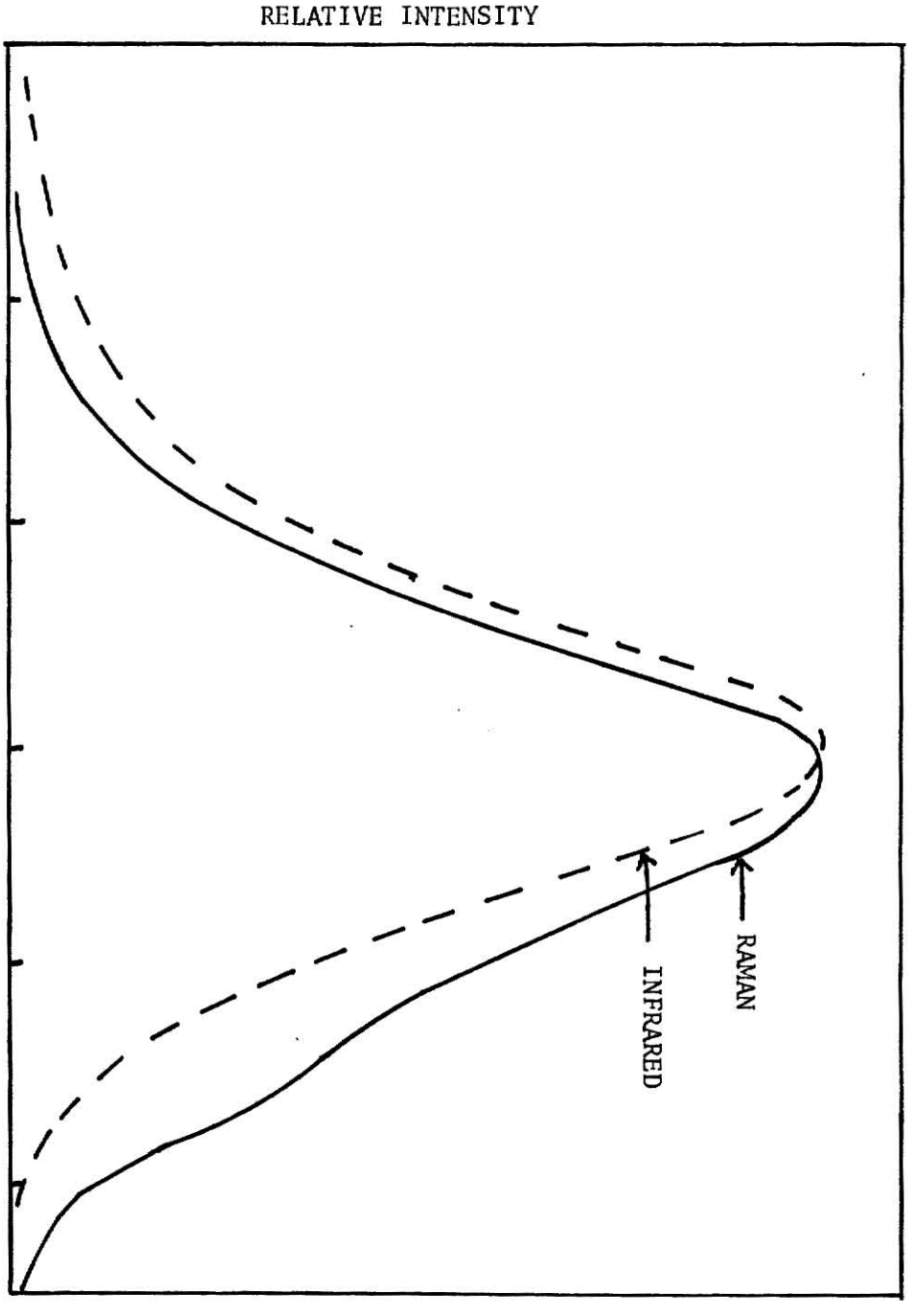
RELATIVE INTENSITY
2300
2400
2500
2600
2700
FREQUENCY (CM^{-1})
INFRARED
RAMAN

FIGURE 18

TABLE I

Prediction of the occurrence of the peak of the shoulder on ν_1 of HDO

The average half-width of the shoulder is 85 ± 15 cm^{-1}	
Temperature (° C)	Position of the Peak (cm^{-1})
25	2635 ± 15
50	2675 ± 15
100	2745 ± 15

TABLE II

Estimates of the "broken hydrogen bonds" in water [6]

Authors	% Estimated	T (°C)	Experimental Basis
Buijs and Choppin [93]	46	0	Near infrared
Cross, Burnham, and Leighton [91]	50	26	Raman spectrum
Danford and Levy [46]	20	25	X-ray diffraction
Davis and Litovitz [98]	18	0	Volume
Eucken [31]	66	0	Ultrasonic absorption
Ewell and Eyring [92]	46	0	Viscosity
Fox and Martin [89]	60	0	Infrared spectrum
Goldstein and Penner [95]	32	0	Near infrared
Grjotheim and Krogh-Moe [32]	56	0	Volume
Haggis, Hasted, and Buchanan [100]	9	0	Dielectric constant
Hall [96]	30	0	Ultrasonic absorption
Litovitz and Carnevale [88]	71.5	0	Ultrasonic absorption
Luck [40]	9-16	0	Near infrared
Marchi and Eyring [30]	2.5	0	Volume
Nemethy and Scheraga [26]	47	0	Structural model
Nomoto [33]	17.5	20	Ultrasonic absorption
Pauling [36]	28.5		Structural model
Pauling [102]	15	0	Heat of melting
Stevenson [101]	0.1	25	Far ultraviolet
Wada [37]	57.5	0	Volume
Walrafen [99]	10.5	0	Dielectric constant

The main reason for the absence of the overtones in the infrared spectra has to do with the contribution of the oscillating dipole moment. Though symmetry considerations do not forbid the presence of these overtones in the infrared spectra, the change in the normal component of the dipole moment is very small. But, in the case of Raman spectra, all that is involved is the derivative of polarizability, which is evidently not as small.

On the Distribution of Hydrogen-Bond Strengths in Water:

The band profiles of HDO are found to be broad, smooth, and single-peaked. So must be the hydrogen bond strengths in liquid water. However the distortion caused by, a) the variation of transmittance of molecules with frequency across the band [15, 81], b) the possible broadening of the band due to short lifetimes of the hydrogen bonds in the liquid, and c) the possible effect on the band intensity of combinations involving the continuum of low-frequency intermolecular vibrations, must be considered for a rigorous evaluation of the distribution of hydrogen-bond strengths. Falk and Ford [7] have indicated, however, that this distortion is of no noticeable consequence in the first approximation, since a) there is a close correspondence between the infrared and Raman profiles of HDO in water; b) the HDO bands in ice are relatively narrow [7, 105]; and c) the band-widths of HDO are nearly constant over a wide range of temperature [7].

On the Distribution of Geometries and on "Clusters" and "Monomers":

Pople [48] has indicated, that the geometry of the hydrogen bond in water is determined by the O...O distance and by angular parameters involved in the deviation of hydrogen bonds from linearity. The smooth, single-peaked distribution of hydrogen-bond strengths in water, as shown by

infrared spectra, possibly reflects a smooth, single-peaked distribution of geometries. The appearance of the Raman spectra also allows the same inference, since the shoulders can be interpreted to be due to the overtones of ν_T.

However, the fact that several geometrical parameters are involved in a highly intricate way, discourages any quantitative study of the detailed shapes of these hydrogen-bond strengths. Also, it is uncertain [7] as to how the distributions relating to OH...O or OD...O bond-length to bond-strength of HDO in D_2O or H_2O would compare with similar relationships for pure H_2O or D_2O. Nevertheless, even though the nonlinearity of the hydrogen bond was neglected, when we used a rough correlation between O...O distances and the OH stretching force constant, and a distribution of O...O distances derived from X-ray measurements in liquid water, the computed frequency distributions were surprisingly similar to the ones observed in Raman and infrared spectra. Wall and Hornig [8] have reported an experimental support for this.

Our assumption that the H atom lies in line with the O...O atoms is somewhat critical, since the position of the H atom determines the hydrogen bond angle, which influences the strength of the hydrogen bond.

There is no unanimity of opinion, in the school of Mixture Models, regarding the percentage of broken hydrogen bonds in water (Table II). Every one, in this school, has his own "operational definition" [101] of what constitutes the rupture of a hydrogen bond. As Table II shows, the estimated percentage varies from 0.1 to 71.5. But the very basic assumption of the mixture models is that the hydrogen bonds in water at any instant can be divided into "broken" and "unbroken" bonds, whereas this division seems to be somewhat "arbitrary" [7], in view of the broad, smooth, and single-peaked

distribution of hydrogen-bond strengths. Since the definitions of "monomers" and "clusters" are dependent on that of a broken hydrogen bond, they are also arbitrary. As Falk and Ford [7] have indicated, depending on one's operational definition of a "broken hydrogen bond," the average size of a "cluster" may vary from one to an infinite number of water molecules at any temperature, while the fraction of molecules present as "clusters" may vary from 0 to 1.

Though the occurrence of an isosbestic point is often associated with the existence of an equilibrium of two absorbing species [107], Falk and Wyss [108] have pointed out, that for substances like water, which absorb in the OH stretching region, isosbestic points are a common occurrence and are observed for solids as well as for liquids. There is no equilibrium between H-bonded and non-H-bonded OH groups in solids.

ACKNOWLEDGEMENTS

I wish to record here my heartfelt deep gratitude to Dr. Basil Curnutte, my major advisor, who not only provided the original idea but also gave constant encouragement and useful suggestions throughout the period of this work.

Also, I wish to thank Dr. James Legg, Dr. John Spangler for being on the advisory committee. Dr. Nathan Folland's kind suggestions, in addition to his being on the advisory committee, are gratefully appreciated.

Finally, thanks are also due to The Kansas State University Agricultural Experiment Station for the sponsorship under which this research was carried out.

REFERENCES

1. C. Eckart, Phys. Rev. 47, 552 (1935).
2. E. B. Wilson and J. B. Howard, J. Chem. Phys. 4, 260 (1936).
3. E. O. Salant and J. E. Rosenthal, Phys. Rev. 42, 812 (1932).
4. W. H. Shaffer and H. H. Nielsen, Phys. Rev. 56, 188 (1939).
5. W. H. Shaffer and R. P. Schuman, J. Chem. Phys. 12, 504 (1944).
6. G. E. Walrafen, J. Chem. Phys. 48, 244 (1968).
7. M. Falk and T. A. Ford, Can. J. Chem. 44, 1699 (1966).
8. T. T. Wall and D. F. Hornig, J. Chem. Phys. 43, 2079 (1965).
9. A. H. Narten, M. D. Danford, and H. A. Levy, X-Ray Diffraction Data on Liquid Water in the Temperature Range 4° to 200°C (ORNL-3997, UC-4 Chemistry) (Oak Ridge National Laboratory, Oak Ridge, Tennessee, 1966).
10. A. H. Narten, M. D. Danford, and H. A. Levy, Discuss. Faraday Soc. 43, 97 (1967).
11. T. T. Wall, J. Chem. Phys. 51, 113 (1969).
12. T. T. Wall, J. Chem. Phys. 52, 2792 (1970).
13. R. G. Gordon, J. Chem. Phys. 43, 1307 (1965).
14. N. E. Dorsey, Properties of Ordinary Water Substance (Reinhold Publishing Co., New York, 1940).
15. G. C. Pimentel and A. L. McClellan, The Hydrogen Bond (W. H. Freeman and Co., San Francisco, 1960).
16. J. L. Kavanau, Water and Solute Water Interactions (Holden-Day, Inc., San Francisco, 1964).
17. W. Luck, Fortschr. Chem. Forsch. 4, 653 (1964).
18. H. S. Frank, Federation Proc., Suppl. No. 15, 24, S-1 (1965).
19. G. Nemethy, Federation Proc., Suppl. No. 15, 24, 38 (1965).
20. O. Y. Samoilov and T. A. Nosova, Zh. Strukt. Khim. 6, 798 (1965) (An English translation (UDC 532.7) is available from the Consultants Bureau, New York).

21. H. Eyring and M. S. Jhon, Chemistry 39, 8 (1966).

22. C. J. Safford, A. W. Naumann, and P. C. Schaffer, A Neutron Scattering Study of Water and Ionic Solutions (Union Carbide Corporation Report, Tuxedo, New York, 1968).

23. H. M. Chadwell, Chem. Rev. 4, 375 (1927).

24. G. R. Choppin, Chemistry 38, 7 (1965).

25. A. Cabana and C. Jolicoeur, Can. Spectry. 12, 94 (1967).

26. G. Nemethy and H. A. Scheraga, J. Chem. Phys. 36, 3382 (1962).

27. W. K. Roentgen, Ann. Phys. Chim. (Wied) 45, 91 (1892).

28. H. S. Frank, Federation Proc. 24, No. 2, Part III. Suppl. No. 15, 1 (1965).

29. O. Y. Samoilov, Die Struktur von Wässrigen Elektrolytlösungen (Teubner Verlag, Leipzig, 1961).

30. R. P. Marchi and H. Eyring, J. Chem. Phys. 38, 221 (1964).

31. A. Eucken, Z. Elektrochem. 52, 255 (1948).

32. K. Grjotheim and J. Krogh-Moe, Acta Chem. Scand. 8, 1193 (1954).

33. O. Nomoto, J. Phys, Soc. Japan, 11, 1146 (1956).

34. H. S. Frank and W. Y. Wen, Discuss. Faraday Soc. 24, 133 (1957).

35. H. S. Frank, Proc. Roy. Soc. London, Ser. A, 247, 481 (1958).

36. L. Pauling, Hydrogen Bonding (Pergamon Press, New York, 1959) p. 1.

37. G. Wada, Bull. Chem. Soc. Japan, 34, 955 (1961).

38. H. S. Frank, Desalination Research Conference Proceedings, Washington. (NAS-NRC publication no. 932, 141 (1963).

39. I. Pelah and J. Imry, Israel Atomic Energy Commission, publication no. 1A-875 (1963).

40. W. Luck, Ber. Bunsenges Physik. Chem. 67, 186 (1963).

41. G. Nemethy and H. A. Scheraga, J. Phys. Chem. 41, 680 (1964).

42. W. Luck, Ber. Bunsenges Physik. Chem. 69, 626 (1965).

43. V. Vand and W. A. Senior, J. Chem. Phys. 43, 1869, 1873 (1965).

44. A. Ben-Naim, J. Phys. Chem. 69, 1922, 3240 (1965).

45. C. M. Davis and T. A. Litovitz, J. Chem. Phys. 42, 2563 (1965).

46. M. D. Danford and H. A. Levy, J. Am. Chem. Soc. 84, 3965 (1962).

47. J. Lennard-Jones and J. A. Pople, Proc. Roy. Soc. London, Ser. A, 205, 155 (1951).

48. J. A. Pople, Proc. Roy. Soc. London, Ser. A, 205, 163 (1951).

49. D. N. Glew, J. Phys, Chem. 66, 605 (1962).

50. C. Tanford, Temperature-its measurement and control in science and industry, Vol. 3 (Reinhold Publishing Corp., New York, 1963) p. 123.

51. J. A. Barker, Ann. Rev. Phys. Chem. 14, 2145 (1965).

52. J. D. Bernal and R. H. Fowler, J. Chem. Phys. 1, 515 (1933).

53. B. T. Darling and D. M. Dennison, Phys. Rev. 57, 128 (1940).

54. F. N. Bjerrum, Verh. d. D. Phys. Ges. 16, 737 (1914).

55. D. M. Dennison, Phil. Mag. 1, 195 (1926).

56. M. Allavena and S. Bratoz, J. Chem. Phys. 60, 1169, (1963).

57. A. Adel and D. M. Dennison, Phys. Rev. 43, 716 (1933); 44, 99 (1933).

58. A. H. Nielsen, J. Chem. Phys. 11, 160 (1943).

59. W. F. Libby, J. Chem. Phys. 11, 101 (1943).

60. J. Schiffer and D. F. Hornig, J. Chem. Phys. 49, 4150 (1968).

61. Y. P. Varshni, Rev. Mod. Phys. 29, 664 (1957).

62. E. R. Lippincott and R. Schroeder, J. Chem. Phys. 23, 1099 (1955).

63. R. Schroeder and E. R. Lippincott, J. Phys. Chem. 61, 921 (1957).

64. G. Herzberg, Molecular Spectra and Molecular Structure, Vol. II, (D. Van Nostrand Co., Inc., New York, 1954) pp. 148.

65. J. Greenstadt, Mathematical Methods for Digital Computers, A. Ralston and H. S. Wilf, eds. (John Wiley and Sons, New York, 1960) pp. 84-91.

66. J. B. Bryan, A Normal Coordinate Analysis of the Local Structure of Liquid Water for Interpretation of Far Infrared Spectra (Ph.D. Dissertation, Kansas State University, 1969).

67. C. Singer, A Short History of Scientific Ideas to 1900 (Oxford University Press, London, 1959) pp. 17, 29-30, 54.

68. J. D. Bernal, The State and Movement of Water in Living Organisms, G. E. Fogg, ed. (Academic Press Inc., New York, 1965) pp. 17-32. (Symposia of the Society for Experimental Biology, No. 19).

69. J. B. Conant, Science and Common Sense (Yale University Press, New Haven, Conn., 1951) pp. 191-205.

70. E. C. Markham and C. E. Smith, General Chemistry (The Riverside Press, Cambridge, 1954) pp. 184-186.

71. T. King, Water, Miracle of Nature (The MacMillan Co., New York, 1953) p. 3.

72. J. W. Moskowitz and M. C. Harrison, J. Chem. Phys. 43, 3550 (1965).

73. K. Morokuma and L. Pederson, J. Chem. Phys. 48, 3274 (1968).

74. P. Pulay, Mol. Phys. 18, 473 (1970).

75. P. Pulay, Mol. Phys. 17, 197 (1969).

76. R. A. Fifer and J. Schiffer, J. Chem. Phys. 50, 21 (1969).

77. L. J. Henderson, The Fitness of the Environment (first published by The MacMillan Company, 1913)(Beacon Press, Boston, 1958) pp. 72-132.

78. O. Hechter, Federation Proc., Suppl. No. 15, 24, 91 (1965).

79. Raj K. Dhingra, private communication.

80. R. A. Fifer and J. Schiffer, J. Chem. Phys. 52, 2664 (1970).

81. T. T. Wall and D. F. Hornig, J. Chem. Phys. 43, 2079 (1965).

82. D. Eisenberg and W. Kauzmann, The Structure and Properties of Water (Oxford University Press, 1969) pp. 152, 163, 170.

83. O. Ya. Samoilov, Structure of Aqueous Electrolyte Solutions and the Hydration of Ions (Consultants Bureau, New York, 1965).

84. D. M. Bishop and M. Randic, J. Chem. Phys. 44, 2480 (1966).

85. J. D. Bernal, Proc. R. Soc. A280, 299 (1964).

86. H. R. Wyss and M. Falk, Can. J. Chem. 48, 607 (1970).

87. W. S. Benedict, N. Gailar, and E. K. Plyler, J. Chem. Phys. 24, 1139 (1956).

88. T. A. Litovitz and E. H. Carnevale, J. Apply Phys. 26, 816 (1955).

89. J. J. Fox and A. E. Martin, Proc. Roy. Soc. London, Ser. A, 174, 234 (1940).

90. S. F. Boys, G. B. Cook, C. M. Reeves, and I. Shavitt, Nature 178, 1207 (1956).

91. P. C. Cross, J. Burnham, and P. A. Leighton, J. Am. Chem. Soc. 59, 1134 (1937).

92. R. H. Ewell and H. Eyring, J. Chem. Phys. 5, 726 (1937).

93. K. Buijs and G. R. Choppin, J. Chem. Phys. 39, 2035 (1963).

94. M. R. Thomas, H. A. Scheraga, and E. E. Schrier, J. Phys, Chem. 69, 3722 (1965).

95. R. Goldstein and S. S. Penner, J. Quant, Spectry. Radiative Transfer, 4, 441 (1965).

96. L. Hall, Phys. Rev. 73, 775 (1948).

97. H. S. Frank and A. S. Quist, J. Chem. Phys. 34, 604 (1961).

98. C. M. Davis and T. A. Litovitz, J. Chem. Phys. 42, 2563 (1965).

99. G. E. Walrafen, J. Chem. Phys. 40, 3249 (1964).

100. G. H. Haggis, J. B. Hasted, and T. J. Buchanan, J. Chem. Phys. 20, 1452 (1952).

101. D. P. Stevenson, J. Phys. Chem. 69, 2145 (1965).

102. L. Pauling, The Nature of the Chemical Bond. 2nd ed. (Cornell University Press, Ithaca, N. Y., 1948) p. 304.

103. M. Magat, Discuss. Faraday Soc. 43, 145 (1967).

104. D. A. Draegert, N. W. B. Stone, B. Curnutte, and D. Williams, J. Opt. Soc. Am. 56, 64 (1966).

105. J. E. Bertie and E. Whalley, J. Chem. Phys. 40, 1637 (1964).

106. B. Widom, Science 157, 375 (1967).

107. W. A. Senior and R. E. Verall, J. Phys. Chem. 73, 4242 (1969).

108. M. Falk and H. R. Wyss, J. Chem. Phys. 51, 5727 (1969).

APPENDIX I

Coordinate Transformations for the Bent XY_2 Molecule

Adopt a body-fixed xyz coordinate axes with origin at the centre of mass and orient the frame so that coordinate axes coincide with principal axes of inertia.

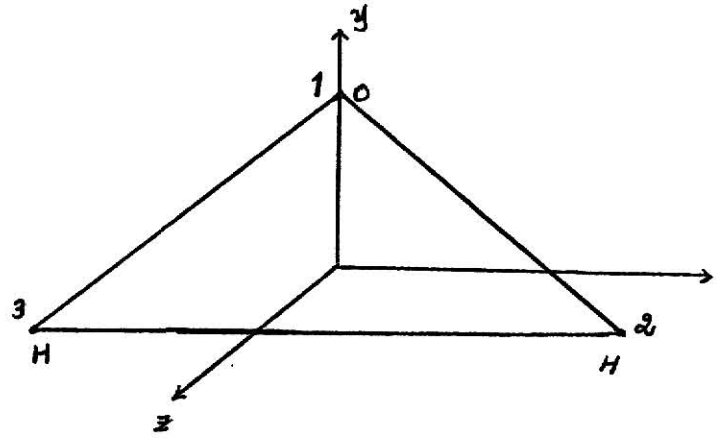

FIG. A-1

The conditions on the original displacement coordinates which enable us to a) separate translations of the whole molecule from vibrations, and to b) separate rotations of the whole molecule from vibrations, are i) origin at the centre of mass:

$$\sum_{n=1}^{3} m_n x_n = \sum_n m_n (x_{on} + x_n') = 0,$$

where the coordinates with subscript 'o' refer to equilibrium values and the ones with primes to displacements of the respective coordinates. We get,

$$\sum_n m_n x_n' = m_1 x_1' + m_2 (x_2' + x_3') = 0 \quad \cdots \quad (1a)$$

$$\sum_n m_n y_n' = m_1 y_1' + m_2 (y_2' + y_3') = 0 \quad \cdots \quad (1b)$$

ii) These are called the Eckart conditions [1, 2].

To zeroth approximation, there is no angular momentum relative to xyz using the equilibrium position of the nuclei as lever arms:

$$\sum_n m_n (\underset{\sim}{r}_{on} \times \underset{\sim}{r}_n') = 0$$

$$\text{i.e.,} \quad \sum_n m_n (x_{on} y_n' - y_{on} x_n') = 0$$

$$\text{Or,} \quad r_o [\mu \cos\alpha_o (-x_1' + \frac{x_2' + x_3'}{2}) + m_2 \sin\alpha_o (y_2' - y_3')] = 0, \quad \cdots (1c)$$

$$\text{where} \quad \mu = \frac{2 m_1 m_2}{(2 m_2 + m_1)} .$$

We need, 3N - 6 = 3, vibrational coordinates. But we have six of them (x_1', x_2', x_3'; y_1', y_2', y_3'). The three non-independent ones can be eliminated using the Eckart conditions.

The approximate combinations as suggested by 1a, 1b, and 1c are [3, 4]:

$$u = x_1' - \frac{1}{2} (x_2' + x_3')$$

$$v = y_1' - \frac{1}{2} (y_2' + y_3')$$

$$w = x_2' - x_3'$$

Combination of 1a, 1b, and 1c with 2a, 2b, and 2c gives

$$\left.\begin{aligned}
x_1' &= \mu u / m_1 \\
x_2' &= -(\mu / 2 m_2) u + w/2 \\
x_3' &= -(\mu / 2 m_2) u - w/2 \\
y_1' &= (\mu / 2 m_2) u \\
y_2' &= -\mu v / 2 m_2 + \mu u \cot\alpha_o / 2 m_2 \\
y_3' &= -\mu v / 2 m_2 - \mu u \cot\alpha_o / 2 m_2
\end{aligned}\right\} \cdots (3)$$

The kinetic energy is [4]

$$T = \frac{1}{2} \sum_n m_n (\dot{x}_n'^2 + \dot{y}_n'^2 + \dot{z}_n'^2)$$

$$= \frac{1}{2} [\mu \dot{s}^2 + \mu_1 \dot{r}^2 + m_2 \dot{w}^2/2],$$

where $$\mu_1 = \mu (1 + \mu \cot^2 \alpha_0 / 2 m_2).$$

Now, let us set up the valence type potential function. From Fig. A-2,

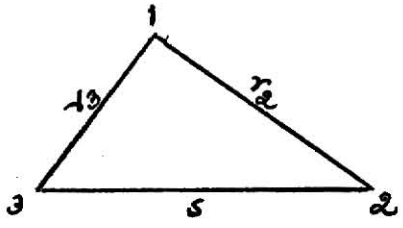

FIG. A-2

$$s^2 = r_2^2 + r_3^2 - 2 r_2 r_3 \cos\beta$$

$$2 s ds = 2 r_2 dr_2 + 2 r_3 dr_3 - 2 (r_2 dr_3 + r_3 dr_2) \cos\beta + 2 r_2 r_3 \sin\beta d\beta$$

$$s s' = r_2 r_2' + r_3 r_3' - (r_2 r_3' + r_3 r_2') \cos\beta + r_2 r_3 \beta' \sin\beta$$

$$s_0 s' = r_{02} r_2' + r_{03} r_3' - (r_{02} r_3' + r_{03} r_3') \cos\beta_0 + r_{02} r_{03} \beta' \sin\beta_0$$

and $$\beta' = [s_0 s' - (r_{02} - r_{03} \cos\beta_0) r_2' - (r_{03} - r_{02} \cos\beta_0) r_3'] / (r_{02} r_{03} \sin\beta_0).$$

For water, $r_{02} = r_{03} = r_0$; $\beta_0 = 2\alpha_0$; and $s_0 = 2 r_0 \sin\alpha_0$, sothat

$$\beta' = [s' - (r_2' + r_3') \sin\alpha_0] / (r_0 \cos\alpha_0)$$

$$= [w \cos\alpha_0 - 2v \sin\alpha_0] / r_0 .$$

Thus, for the valence-type coordinates we have

$$\beta' = [\cos\alpha_o\, w - 2v\sin\alpha_o]/r_o$$

$$r_2' = \tfrac{1}{2} w\sin\alpha_o + v\cos\alpha_o - \mu_1 u\sin\alpha_o/\mu$$

$$r_3' = \tfrac{1}{2} w\sin\alpha_o + v\cos\alpha_o + \mu_1 u\sin\alpha_o/\mu.$$

The complete quadratic "valence-type" potential function is

$$2V = \{C_1(r_2'^2 + r_3'^2) + C_2\beta^2 + C_3\beta(r_2' + r_3') + C_4 r_2' r_3'\}$$

$$= \mathcal{A}u^2 + \mathcal{B}v^2 + \mathcal{C}w^2 + 2\mathcal{D}vw$$

with

$$\mathcal{A} = 2C_1\left(\frac{\mu_1}{\mu}\sin\alpha_o\right)^2 - C_4\left(\frac{\mu_1}{\mu}\sin\alpha_o\right)^2$$

$$\mathcal{B} = 2C_1\cos^2\alpha_o + \frac{4C_2\sin^2\alpha_o}{r_o^2} - 4C_3\frac{\cos\alpha_o\sin\alpha_o}{r_o} + C_4\cos^2\alpha_o$$

$$\mathcal{C} = \tfrac{1}{2}C_1\sin^2\alpha_o + \frac{C_2}{r_o^2}\cos^2\alpha_o + \tfrac{1}{2}C_3\frac{\sin 2\alpha_o}{r_o} + \frac{C_4}{4}\sin^2\alpha_o$$

$$\mathcal{D} = C_1\sin\alpha_o\cos\alpha_o - \frac{2C_2\sin\alpha_o\cos\alpha_o}{r_o^2} + \frac{C_3}{r_o}\cos 2\alpha_o + \frac{C_4}{8}\sin 2\alpha_o$$

APPENDIX II

Kinetic and Potential Energy Expressions for the Bent XYZ Molecule

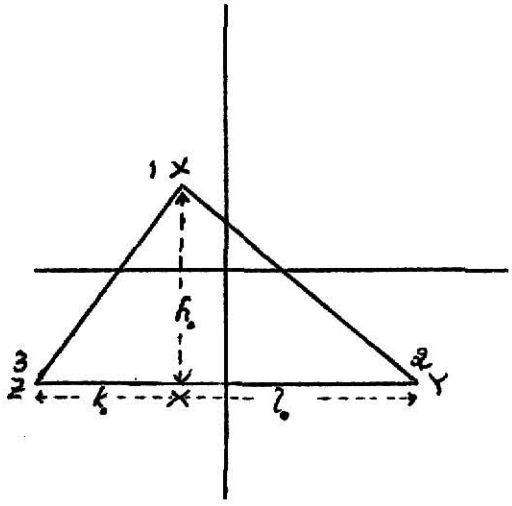

FIG. B-1

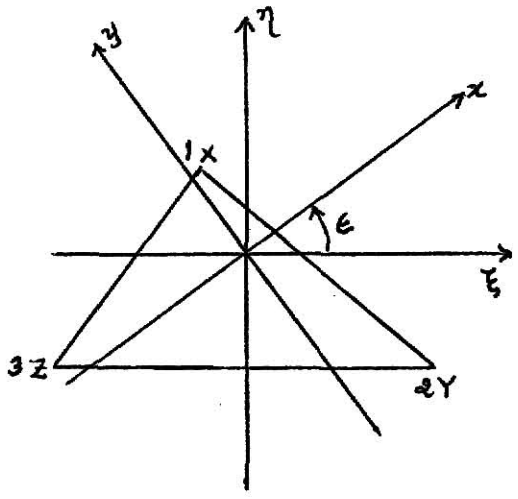

FIG. B-2

The equilibrium configuration of the general bent XYZ molecule, as shown schematically by Fig. B-1, is a triangle of height h_o and base ($k_o + l_o$). The vibrationless positions of the atomic nuclei are specified by a right-handed body-fixed coordinate system (ξ, η, ζ). The molecule lies in the $\eta\xi$-plane. The origin of the coordinates is at the centre of mass of the molecule and the ξ-axis parallel to the base of the triangle [5].

Consider a new set of principal axes of inertia xyz (adopted for the equilibrium configuration in order to facilitate the investigation of interactions between rotation and vibration). The xyz system has its origin at the centre of mass, its z-axis coincident with the ζ-axis, and its xy-axes in the plane of the molecule and making an angle ε with the $\xi\eta$-axes.

The equilibrium values of x_i and y_i are

$$\left.\begin{aligned} x_{oi} &= \xi_{oi}\cos\epsilon + \eta_{oi}\sin\epsilon, \\ y_{oi} &= -\xi_{oi}\sin\epsilon + \eta_{oi}\cos\epsilon, \end{aligned}\right\} \quad \cdots (1)$$

where ϵ is chosen such that the equilibrium value of the product of inertia,

$$I_{exy} = \sum_i m_i x_{oi} y_{oi} \quad , \text{ vanishes.}$$

It follows that [5]

$$\tan 2\epsilon = A/B, \quad \cdots (2)$$

where

$$A = 2m_1 h_o (m_3 k_o - m_2 \ell_o), \quad \cdots (2a)$$

$$B = m_3(m_1+m_2)k_o^2 + m_2(m_1+m_3)\ell_o^2 + 2m_2 m_3 k_o \ell_o - m_1(m_2+m_3)h_o^2 \quad \cdots (2b)$$

The equilibrium values of the principal moments of inertia are

$$\left.\begin{aligned} I_{ex} &= (I_{ez} - I')/2, \\ I_{ey} &= (I_{ez} + I')/2, \\ I_{ez} &= [B + 2m_1(m_2+m_3)h_o^2]/M, \end{aligned}\right\} \quad \cdots (3)$$

where

$$I' = \pm (A^2+B^2)^{1/2}/M.$$

We have to choose a set of 3N - 6 = 3, generalized coordinates with the aid of the Eckart conditions [1, 2]:

$$\left.\begin{aligned} &\sum_i m_i x_i' = 0 \quad , \quad \sum_i m_i y_i' = 0, \\ \text{and} \quad &\sum_i m_i (x_{oi} y_i' - y_{oi} x_i') = 0 \end{aligned}\right\} \quad \cdots (4a)$$

An appropriate set, which reduces in the limiting case to that employed in the XY_2 problem as given in Appendix I, is

$$\left.\begin{aligned} u &= x_1' - [(m_2 x_2' + m_3 x_3')/(m_2+m_3)] \\ v &= y_1' - [(m_2 y_2' + m_3 y_3')/(m_2+m_3)] \\ w &= x_2' - x_3' \end{aligned}\right\} \quad \cdots (4b)$$

From (4a) and (4b),

$$x_1' = \mu u/m_1 ,$$

$$x_2' = -\mu u/(m_2+m_3) + \mu' w/m_2 ,$$

$$x_3' = -\mu u/(m_2+m_3) - \mu' w/m_3 ,$$

$$y_1' = \mu v/m_1 ,$$

$$y_2' = \frac{\mu\alpha}{m_2} v + \frac{\mu''}{m_2} u + \frac{\mu'\gamma}{m_2} w ,$$

and $$y_3' = \frac{\mu\beta}{m_3} v - \frac{\mu''}{m_3} u - \frac{\mu'\gamma}{m_3} w ,$$

where

$$\mu = (m_2+m_3) m_1/M ,$$

$$\mu' = m_2 m_3/(m_2+m_3),$$

$$\alpha = (x_{03}-x_{01})/(x_{02}-x_{03}),$$
$$\beta = (x_{01}-x_{02})/(x_{02}-x_{03}),$$
$$\gamma = (y_{02}-y_{03})/(x_{02}-x_{03}).$$

The kinetic energy

$$T = \frac{1}{2} \sum_i m_i (\dot{x}_i^2 + \dot{y}_i^2 + \dot{z}_i^2)$$

$$= \frac{1}{2}[\mu_{11}\dot{u}^2 + \mu_{22}\dot{v}^2 + \mu_{33}\dot{w}^2 + 2\mu_{12}\dot{u}\dot{v} + 2\mu_{13}\dot{u}\dot{w} + 2\mu_{23}\dot{v}\dot{w}],$$

where

$$\mu_{11} = \mu + (\mu''^2/\mu'), \quad \mu'' = m_1 y_{01}/(x_{02} - x_{03}),$$

$$\mu_{22} = \mu'/m_1 + \frac{\mu''^2\alpha^2}{m_2} + \frac{\mu''^2\beta^2}{m_3},$$

$$\mu_{33} = \mu'(1+\gamma^2),$$

$$(\mu_{12}/\mu'') = (\mu_{23}/\mu'\gamma) = (\mu\frac{\alpha}{m_2}) - \frac{\mu\beta}{m_3},$$

$$\mu_{13} = \mu''\gamma.$$

From FIG. B-3,

$$h_o = r_{02}\cos\alpha_{02} = r_{03}\cos\alpha_{03},$$

$$k_o = r_{03}\sin\alpha_{03}, \quad l_o = r_{02}\sin\alpha_{02},$$

$$\beta_o = \alpha_{02} + \alpha_{03}.$$

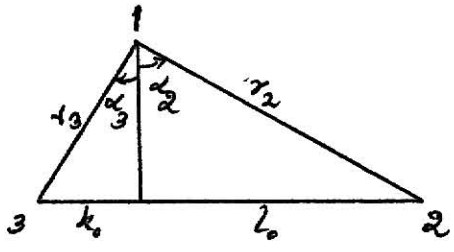

FIG. B-3

Now,

$$r_{02}\cos(\beta_o - \alpha_{03}) = r_{03}\cos\alpha_{03}$$

i.e., $$\sin\beta_o \sin\alpha_{03} = \frac{r_{03}}{r_{02}}\cos\alpha_{03} - \cos\beta_o\cos\alpha_{03},$$

or, $$\tan\alpha_{03} = \left(\frac{r_{03}}{r_{02}}\frac{1}{\sin\beta_o} - \cot\beta_o\right),$$

so that

$$\alpha_{03} = \tan^{-1}\left[\frac{r_{03}}{r_{02}}\frac{1}{\sin\beta_o} - \cot\beta_o\right].$$

The equilibrium coordinates are given by [5]

$$x_{01} = (m_3 k_0 - m_2 \ell_0)\frac{\cos\epsilon}{M} + (m_2+m_3)\frac{h_0}{M}\sin\epsilon$$

$$x_{02} = [(m_3 k_0 + (m_1+m_3)\ell_0]\frac{\cos\epsilon}{M} - \frac{m_1 h_0}{M}\sin\epsilon$$

$$x_{03} = -[(m_1+m_2)k_0 + m_2\ell_0]\frac{\cos\epsilon}{M} - \frac{m_1 h_0}{M}\sin\epsilon$$

$$y_{01} = (m_2\ell_0 - m_3 k_0)\frac{\sin\epsilon}{M} + (m_2+m_3)h_0\frac{\cos\epsilon}{M}$$

$$y_{02} = -[m_3 k_0 + (m_1+m_3)\ell_0]\frac{\sin\epsilon}{M} - \frac{m_1 h_0}{M}\cos\epsilon$$

$$y_{03} = [m_2\ell_0 + (m_1+m_2)k_0]\frac{\sin\epsilon}{M} - \frac{m_1 h_0}{M}\cos\epsilon.$$

Also, $s_0^2 = r_{02}^2 + r_{03}^2 - 2 r_{02} r_{03}\cos\beta_0.$

Writing

$$r_2^2 = (r_{02} + r_2')^2,$$

we get, $r_2^2 = (x_2 - x_1)^2 + (y_2 - y_1)^2$

$$= (x_{02} - x_{01})^2 + (x_2' - x_1')^2 + 2(x_{02} - x_{01})(x_2' - x_1')$$
$$+ (y_{02} - y_{01})^2 + (y_2' - y_1')^2 + 2(y_{02} - y_{01})(y_2' - y_1');$$

and

$$\delta\beta_0 = [s_0 s' - (r_{02} - r_{03}\cos\beta_0)r_2' - (r_{03} - r_{02}\cos\beta_0)r_3']/(r_{02} r_{03}\sin\beta_0).$$

Comparing terms,

$$r_2' = \frac{1}{r_{02}}[(x_{02} - x_{01})(x_2' - x_1') + (y_{02} - y_{01})(y_2' - y_1')],$$

$$r_3' = \frac{1}{r_{03}}[(x_{03} - x_{01})(x_3' - x_1') + (y_{03} - y_{01})(y_3' - y_1')],$$

$$s' = \frac{1}{s_0}[(x_{03} - x_{02})(x_3' - x_2') + (y_{03} - y_{02})(y_3' - y_2')].$$

Putting for primed coordinates on the right hand sides,

$$r_2' = \mathcal{A}_1 u + \mathcal{A}_2 v + \mathcal{A}_3 w,$$
$$r_3' = \mathcal{B}_1 u + \mathcal{B}_2 v + \mathcal{B}_3 w,$$
$$s' = \mathcal{D}_1 u + \mathcal{D}_2 v + \mathcal{D}_3 w,$$
$$\beta' = \mathcal{C}_1 u + \mathcal{C}_2 v + \mathcal{C}_3 w,$$

where

$$\mathcal{A}_1 = [x_{012} - \mu''(y_{012}/m_2)]/r_{02},$$
$$\mathcal{A}_2 = [x_{013} + \mu'' y_{013}/m_3]/r_{03},$$
$$\mathcal{A}_3 = -\mu(x_{012} + \gamma y_{012})/(r_{02} m_2),$$
$$\mathcal{B}_1 = [x_{013} + \mu'' y_{013}/m_3]/r_{03},$$
$$\mathcal{B}_2 = \mu y_{013}[1/m_1 - \beta/m_3]/r_{03},$$
$$\mathcal{B}_3 = (\mu'/m_3)[x_{013} + \gamma y_{013}]/r_{03},$$
$$\mathcal{C}_1 = [s_0 \mathcal{D}_1 - (r_{02} - r_{03}\cos\beta_0)\mathcal{A}_1 - (r_{03} - r_{02}\cos\beta_0)\mathcal{B}_1]\cos\alpha_{03}/(r_{02}\sin\beta_0),$$
$$\mathcal{C}_2 = [s_0 \mathcal{D}_2 - (r_{02} - r_{03}\cos\beta_0)\mathcal{A}_2 - (r_{03} - r_{02}\cos\beta_0)\mathcal{B}_2]\cos\alpha_{03}/(r_{02}\sin\beta_0),$$
$$\mathcal{C}_3 = [s_0 \mathcal{D}_3 - (r_{02} - r_{03}\cos\beta_0)\mathcal{A}_3 - (r_{03} - r_{02}\cos\beta_0)\mathcal{B}_3]\cos\alpha_{03}/(r_{02}\sin\beta_0),$$
$$\mathcal{D}_1 = \mu'' y_{023}/(\mu' s_0),$$
$$\mathcal{D}_2 = \mu y_{023}[\alpha/m_2 - \beta/m_3]/s_0,$$
$$\mathcal{D}_3 = [x_{023} + \gamma y_{023}]/s_0.$$

The notation used is $x_{012} = x_{01} - x_{02}$, $y_{023} = y_{02} - y_{03}$, etc.

The complete potential function is

$$2V = c_{12} r_2'^2 + c_{13} r_3'^2 + c_2 \beta'^2 + 2c_3 \beta'(r_2' + r_3') + 2c_4 r_2' r_3'$$
$$= k_{11} u^2 + k_{22} v^2 + k_{33} w^2 + 2k_{12} uv + 2k_{23} vw + 2k_{31} wu,$$

where

$$k_{ij} = [(\mathcal{A}_i \mathcal{A}_j) c_{12} + (\mathcal{B}_i \mathcal{B}_j) c_{13} + \mathcal{C}_i \mathcal{C}_j c_2 + \{(\mathcal{A}_i + \mathcal{B}_i)\mathcal{C}_j + (\mathcal{A}_j + \mathcal{B}_j)\mathcal{C}_i\} c_3 + (\mathcal{A}_i \mathcal{B}_j + \mathcal{A}_j \mathcal{B}_i) c_4].$$

APPENDIX III

The symmetric T-matrix was diagonalized to get the eigenvalues k_1, k_2, k_3, and the eigenvectors-matrix P.

That is,

$$P'TP = \begin{pmatrix} k_1 & 0 & 0 \\ 0 & k_2 & 0 \\ 0 & 0 & k_3 \end{pmatrix}$$

If

$$R \equiv P \begin{pmatrix} \frac{1}{\sqrt{k_1}} & 0 & 0 \\ 0 & \frac{1}{\sqrt{k_2}} & 0 \\ 0 & 0 & \frac{1}{\sqrt{k_3}} \end{pmatrix}$$

then

$$R'TR = \begin{pmatrix} \frac{1}{\sqrt{k_1}} & 0 & 0 \\ 0 & \frac{1}{\sqrt{k_2}} & 0 \\ 0 & 0 & \frac{1}{\sqrt{k_3}} \end{pmatrix} \begin{pmatrix} & P'TP & \end{pmatrix} \begin{pmatrix} \frac{1}{\sqrt{k_1}} & 0 & 0 \\ 0 & \frac{1}{\sqrt{k_2}} & 0 \\ 0 & 0 & \frac{1}{\sqrt{k_3}} \end{pmatrix}$$

$$= \begin{pmatrix} \frac{1}{\sqrt{k_1}} & 0 & 0 \\ 0 & \frac{1}{\sqrt{k_2}} & 0 \\ 0 & 0 & \frac{1}{\sqrt{k_3}} \end{pmatrix} \begin{pmatrix} k_1 & 0 & 0 \\ 0 & k_2 & 0 \\ 0 & 0 & k_3 \end{pmatrix} \begin{pmatrix} \frac{1}{\sqrt{k_1}} & 0 & 0 \\ 0 & \frac{1}{\sqrt{k_2}} & 0 \\ 0 & 0 & \frac{1}{\sqrt{k_3}} \end{pmatrix}$$

$$= I.$$

APPENDIX IV

```
      DIMENSION T(9),SMU(9),PA(3),PB(3),PC(3),PD(3),L(9),W(9),
     1Y(9),BAY(3,3),Q(9),TMP(9),FN(9),RPR(9),RS(9),RP(9),S(9),FK(9)
      DIMENSIONR(101),RFL(101),SKH(101),CA(101),CB(101),CC(101),HT(101),
     1H(101),MRD(4000),BX(1500,3),FKN(9),FP(9)
C     THIS PROGRAM IS FOR HDO FREQUENCY DISTRIBUTION(BANDEKAR JAGDEESH).
    3 FORMAT(1H1)
    5 FORMAT(25(I2),30X)
    6 FORMAT(4(E16.8))
   14 FORMAT(I2)
   42 FORMAT(3(I4))
   97 FORMAT(3(E9.3))
   98 FORMAT(3(E10.4))
  101 FORMAT(3(E11.4))
  102 FORMAT(3(E11.4))
  105 FORMAT(E11.4)
  300 FORMAT(3(E11.4))
  301 FORMAT(4(E11.4))
      READ(1,300)AF,BF,CF
      READ(1,98)RFLMN,RFLMX,RFLCR
      READ(1,101)WM1,WM2,WM3
      READ(1,102)BKH,SBH,SSKH
      READ(1,105)BETA
      WRITE(3,3)
C     PART  ONE: GET SKH(I) AS A FUNCTION OF RFL(I).
      FINC=(RFLMX-RFLMN)/100
      C=(1.18)*(6.947281E-12)
      DN=4.59E+08
      DNN=6.66E+08
C     THIS DEFINES OUR FORCE CONSTANT.
      CC(I)=EXP(-DN*(R(I)-RO)*(R(I)-RO)/R(I))
      RO=.97E-08
      DD=5.6533E-12
      DO503I=1,101
      FFI=FLOAT(I)
      RFL(I)=RFLMN+(FFI-1.)*FINC
      IF(I.EQ.1)R(I)=1.0E-08
      IF(I.NE.1)R(I)=R(I-1)
  501 RDIF1=RFL(I)-R(I)
      RDIF2=RDIF1*RDIF1
      RR=RO+(1.-RO*RO/RDIF2)*R(I)*R(I)*EXP(-DNN*(RDIF1-RO)*
     1(RDIF1-RO)/RDIF1+DN*(R(I)-RO)*(R(I)-RO)/R(I))/(R(I)+RO)
      DIFF=ABS(RR-R(I))
      R(I)=(RR+R(I))/2.
      IF(DIFF.LT..5E-13)GOTO502
      GOTO501
  502 CONTINUE
      CA(I)=EXP(-DNN*(RDIF1-RO)*(RDIF1-RO)/RDIF1)
      CB(I)=1.-RO*RO/RDIF2
      SKH(I)=(2*DN*C*CC(I)/(R(I)**3))*(RO**2-(DN*(R(I)-RO)*
```

```
     1(R(I)-RO)*(R(I)+RO)*(R(I)+RO)/(2*(R(I))))+(2*DNN*DD*CA(I)/
     1(RDIF1**3))*(RO**2-(DNN*(RDIF1-RO)*(RDIF1-RO)*(RDIF1+RO)*
     1(RDIF1+RO)/(2*RDIF1)))
  503 CONTINUE
      DO57I=1,101
      IF(RFL(I)-RFLCR)55,56,56
   55 HT(I)=(2.*(RFL(I)-RFLMN))/((RFLMX-RFLMN)*(RFLCR-RFLMN))
      GOTO57
   56 HT(I)=(2.*(RFLMX-RFL(I)))/((RFLMX-RFLMN)*(RFLMX-RFLCR))
   57 CONTINUE
      HSUM=0.
      DO58I=1,101
      HSUM=HSUM+HT(I)
   58 CONTINUE
      DO59I=1,101
      H(I)=HT(I)/HSUM
   59 CONTINUE
      CV=2.997925E10
      PI=3.1415927E00
C     INITIALIZE "BOXES".
      DO810M=1,1500
      DO809N=1,3
  809 CONTINUE
      BX(M,N)=0
  810 CONTINUE
C     RANDOM NUMBERS ARE GENERATED HERE.
      IX=81143
      DO 999 I=1,2000
      CALL RANDU(IX,IY,YFL)
      MRD(I)=100.*YFL
      IX=IY
  999 CONTINUE
C     FREQUENCY DISTRIBUTION PART.
      DO 998 JM=1,1000
      JJ=(JM-1)*2
      J1=MRD(JJ+1)
      J2=MRD(JJ+2)
      SKH2=SKH(J1+1)
      SKH3=SKH(J2+1)
      RO2=R(J1+1)
      RO3=R(J2+1)
      H1=H(J1+1)
      H2=H(J2+1)
      PHT=H1*H2
C     PART TWO: GET PROBABILITY AS A FUNCTION OF FREQUENCY.
      SMS=WM1+WM2+WM3
      AMU=((WM2+WM3)*WM1)/SMS
      AMUP=(WM2*WM3)/(WM2+WM3)
      TAT=(RO3/(RO2*SIN(BETA)))-(COTAN(BETA))
      ALP3=ATAN(TAT)
```

```
      ZL=RO2*SIN(BETA-ALP3)
      ZK=RO3*SIN(ALP3)
      ZH=RO3*COS(ALP3)
      PZO=RO3*SIN(ALP3)+RO2*SIN(BETA-ALP3)
      SME=2.*WM1*RO3*COS(ALP3)*(WM3*RO3*SIN(ALP3)-WM2*RO2*
     1SIN(BETA-ALP3))
      SNE=WM3*(WM1+WM2)*((RO3*SIN(ALP3))**2)+WM2*(WM1+WM3)*
     1((RO2*SIN(BETA-ALP3))**2)+2*WM2*WM3*RO2*RO3*SIN(ALP3)*
     1SIN(BETA-ALP3)-WM1*(WM2+WM3)*((RO3*COS(ALP3))**2)
      SMNE=SME/SNE
      EPS2=ATAN(SMNE)
      EPS=EPS2/2.
      XO1=((((WM3*ZK)-(WM2*ZL))*COS(EPS))+(WM2+WM3)*ZH*SIN(EPS))/SMS
      XO2=(((WM3*ZK+(WM1+WM3)*ZL)*COS(EPS))-(WM1*ZH*SIN(EPS)))/SMS
      XO3=-((((WM1+WM2)*ZK)+(WM2*ZL))*COS(EPS)+(WM1*ZH*SIN(EPS)))/
     1SMS
      YO1=(((WM2*ZL-WM3*ZK)*SIN(EPS))+(WM2+WM3)*ZH*COS(EPS))/SMS
      YO2=-(((WM3*ZK+(WM1+WM3)*ZL)*SIN(EPS))+(WM1*ZH*COS(EPS)))/SMS
      YO3=((WM2*ZL+(WM1+WM2)*ZK)*SIN(EPS)-(WM1*ZH*COS(EPS)))/SMS
      XO31=XO3-XO1
      XO13=-XO31
      XO21=XO2-XO1
      XO12=-XO21
      XO32=XO3-XO2
      XO23=-XO32
      YO31=(YO3-YO1)
      YO13=-YO31
      YO21=YO2-YO1
      YO12=-YO21
      YO23=YO2-YO3
      YO32=-YO23
      AMUPP=(WM1*YO1)/XO23
      AC=XO31/XO23
      BC=XO12/XO23
      GC=YO23/XO23
      SMU(1)=AMU+((AMUPP**2)/AMUP)
      SMU(2)=(AMU*AMUPP*(AC/WM2))-(AMU*AMUPP*(BC/WM3))
      SMU(3)=((AMU**2)/WM1)+((AMU**2)*(AC**2)/WM2)+
     1((AMU**2)*(BC**2)/WM3)
      SMU(4)=AMUPP*GC
      SMU(5)=(AMU*AMUP*AC*(GC/WM2))-(AMU*AMUP*BC*(GC/WM3))
      SMU(6)=AMUP*(1.+GC**2)
      PA(1)=(XO12-AMUPP*YO12/WM2)/RO2
      PA(2)=AMU*YO12*((1./WM1)-(AC/WM2))/RO2
      PA(3)=-AMUP*(XO12+GC*YO12)/(RO2*WM2)
      PB(1)=(XO13+AMUPP*YO13/WM3)/RO3
      PB(2)=AMU*YO13*((1./WM1)-(BC/WM3))/RO3
      PB(3)=AMUP*(XO13+GC*YO13)/(RO3*WM3)
      PD(1)=AMUPP*YO23/(PZO*AMUP)
      PD(2)=AMU*YO23*((AC/WM2)-(BC/WM3))/PZO
```

```
      PD(3)=(XO23+GC*YO23)/PZO
      PC(1)=(PZO*PD(1)-(RO2-RO3*COS(BETA))*PA(1)-(RO3-RO2*
     1COS(BETA))*PB(1))*COS(ALP3)/(RO2*SIN(BETA))
      PC(2)=(PZO*PD(2)-(RO2-RO3*COS(BETA))*PA(2)-(RO3-RO2*
     1COS(BETA))*PB(2))*COS(ALP3)/(RO2*SIN(BETA))
      PC(3)=(PZO*PD(3)-(RO2-RO3*COS(BETA))*PA(3)-(RO3-RO2*
     1COS(BETA))*PB(3))*COS(ALP3)/(RO2*SIN(BETA))
      DO1101I=1,3
      DO 1102 LL=1,3
      BAY(I,LL)=(PA(I)*PA(LL)*SKH2)+(PB(I)*PB(LL)*SKH3)+(PC(I)*PC(LL)*
     1BKH)+((PA(I)+PB(I))*PC(LL)+(PA(LL)+PB(LL))*PC(I))*SBH+
     1(PA(I)*PB(LL)+PA(LL)*PB(I))*SSKH
1102  CONTINUE
1101  CONTINUE
      Y(1)=BAY(1,1)
      Y(5)=BAY(2,2)
      Y(9)=BAY(3,3)
      Y(2)=BAY(2,1)
      Y(4)=BAY(1,2)
      Y(3)=BAY(3,1)
      Y(7)=BAY(1,3)
      Y(6)=BAY(3,2)
      Y(8)=BAY(2,3)
      CALL EIGEN(SMU,Q,3,0)
      S(1)=SMU(1)
      S(2)=SMU(3)
      S(3)=SMU(6)
      DO81I=1,3
      RP(I)=(1./(SQRT(S(1))))*Q(I)
   81 CONTINUE
      DO 78 LM=4,6
      RP(LM)=(1./(SQRT(S(2))))*Q(LM)
   78 CONTINUE
      DO79K=7,9
      RP(K)=(1./(SQRT(S(3))))*Q(K)
   79 CONTINUE
      CALL GMTRA(RP,RPR,3,3)
      CALL GMPRD(RPR,Y,TMP,3,3,3)
      CALL GMPRD(TMP,RP,FN,3,3,3)
      FK(1)=FN(1)
      FK(2)=FN(4)
      FK(3)=FN(5)
      FK(4)=FN(7)
      FK(5)=FN(8)
      FK(6)=FN(9)
      CALL EIGEN(FK,W,3,1)
      FP(1)=FK(1)
      FP(2)=FK(3)
      FP(3)=FK(6)
      DO10I=1,3
```

```
      FKN(I)=(SQRT(FP(I)))/(2.*CV*PI)
   10 CONTINUE
      DO899I=1,3
      FFF=FKN(I)+1
  899 CONTINUE
      GO TO(301,302,303),I
  301 FFF=FFF-AF
      GOTO 310
  302 FFF=FFF-BF
      GOTO 310
  303 FFF=FFF-CF
  310 NBX=FFF
      IF(NBX.LT.1)GOTO 811
      IF(NBX.GT.1500)GOTO 811
      BX(NBX,I)=BX(NBX,I)+PHT
      GOTO 899
  811 CONTINUE
      WRITE(3,880)I,NBX
  880 FORMAT(5X,12HOUT OF RANGE,3X,14HFREQUENCY NO= ,I1,
     15HBOX= ,I4,3X)
  998 CONTINUE
      DO 813I=1,1500
  813 WRITE(3,814)I,(BX(I,J),J=1,3)
  814 FORMAT(2X,I4,2X,3(E16.8,4X))
      WRITE(3,97)AF,BF,CF
      WRITE(3,97)RFLMN,RFLCR,RFLMX
      STOP
      END
```

VITA

JAGDEESHCHANDRA NARAYANRAO BANDEKAR

Candidate for the Degree of Master of Science

Thesis: THE INTRAMOLECULAR VIBRATIONS OF THE WATER MOLECULE IN THE LIQUID STATE

Major field: Physics

Biographical:

Personal data: Born in Alnavar, Mysore, India, October 19, 1946, the son of Shri and Smt. Narayanrao Yeshwantrao Bandekar.

Education: Attended K. B. School, Alnavar; graduated from the Basel Mission Higher Secondary School, Dharwar in 1963; received the Bachelor of Science degree from Karnatak College, Dharwar, with a major in Physics in 1967; received the Master of Science degree with a specialization in Nuclear physics from Karnatak University, Dharwar, in August 1969; completed requirements for Master of Science degree of Kansas State University in August 1970.

THE INTRAMOLECULAR VIBRATIONS OF THE WATER MOLECULE IN THE LIQUID STATE

by

JAGDEESHCHANDRA N. BANDEKAR

M.Sc., Karnatak University, Dharwar, India, 1969

AN ABSTRACT OF A MASTER'S THESIS

submitted in partial fulfillment of the

requirements for the degree

MASTER OF SCIENCE

Department of Physics

KANSAS STATE UNIVERSITY
Manhattan, Kansas

1970

ABSTRACT

Recently observed infrared and Raman spectra have provided very interesting data which have been interpreted reasonably well in terms of two entirely different models of liquid water. A normal coordinate analysis based on a continuum model of a general XYZ molecule is used to study the frequency distribution due to vibrational motions of water molecule in the liquid state. The vibrational spectra are converted into distribution functions by taking the height of the band at each frequency as a measure of the number of oscillators having that frequency at any instant. Of the five adjustable parameters in the potential energy function, the first two (C_{12}, C_{13}) are chosen from the papers due to Lippincott and Schroeder [1, 2], while the rest three are determined from H_2O, HDO, and D_2O infrared data. The X-ray pair correlation functions [3] give a distribution of equilibrium O-O distances at various temperatures. The occurrence of shoulders in the Raman spectra is interpreted for the first time on a reasonably quantitative basis as being due to the combinations with the translational bands. Thus, our five parameter potential function reproduces the observed frequency distribution [4], and hence lends support to the Continuum Model.

1. E. R. Lippincott and R. Schroeder, J. Chem. Phys. 23, 1099 (1955).

2. R. Schroeder and E. R. Lippincott, J. Chem. Phys. 61, 921 (1957).

3. A. H. Narten, M. D. Danford, and H. A. Levy, X-Ray Diffraction Data on Liquid Water in the Temperature Range 4° to 200° C (ORNL-3997, UC-4 Chemistry) (Oak Ridge National Laboratory, Oak Ridge, Tennessee, 1966).

4. H. R. Wyss and M. Falk, Can. J. Chem. 48, 607 (1970).